Design of Visualization Tool for Biomechanical Rowing Analysis

A Major Qualifying Project
Submitted to the Faculty of
WORCESTER POLYTECHNIC INSTITUTE
In partial fulfillment for the
Degree of Bachelor of Science

By:

Josephine Bowen
Blake Dobay
Marc Reardon
Ben Thornton

Date: May 5, 2020

Report Submitted to:

Tiffiny Butler, PhD ATC , Advisor
Lane Harrison, Co-Advisor
Selcuk Guceri, Co-Advisor
Jon Rourke, Sponsor

Table of contents

Table of figures

Table of tables

Glossary

Ergometer (erg): stationary rowing machine
Shell: the hull of a rowing boat
Eight: a rowing boat that hold eight rowers and a coxswain
Coxswain: an individual who sits in the stern of the boat and steers
Head race: boats race in single file and compete against the clock
Sweeping: a style of rowing where rowers each use one oar
Sculling: a style of rowing where rowers each use two oars
Catch: the position where the rower reaches the front of the slide
Drive: the power portion of the stroke, the leg drive
Finish: the final part of the drive, handle is pulled into body
Recovery: rower moves from the finish back to the catch
Starboard: a rower whos oar is on their left side
Port: a rower whos oar is on their left side

Abstract

Performance in rowing is reliant on the precise and consistent execution of strokes. Perfection of the stroke takes years of focused effort, with particular focus on the timing of the legs, trunk and arms. Training is required not only on the water but on stationary training ergometers. Currently, instrumentation of the rowing stroke timing elements is limited to rating and coaching feedback. There is still no componitized feedback system for the three main elements of the stroke: legs, body, arms. This project's aim is to create a visualization tool for rowers that breaks down the three movements in the stroke to provide coachable feedback. The tool has three microelectromechanical system (MEMS) sensors, each of which is positioned corresponding to the targeted movement. The first sensor is located on the seat of the erg, the second on the handle, and the last sensor on the rower's back. A display of the rower's timing element data allows them to learn and correct their strokes in real time. The system is still in development so it has a few limitations. A bad connection from the tape inhibited data transfer so heavy interpolation was used. Underfitting is likely. Possible future routes for this project include using machine learning to determine stroke quality, using machine learning to detect the phases of the stroke, engineering a wearable holder for the sensors to improve data transfer, and developing better ways to visualize the stroke in real time.

Executive Summary

The ergometer (erg) has become one of the most useful tools for the general rower, it allows an athlete to receive live feedback on speed, power application, and stroke rate over time. This allows experienced athletes to gather data related to the power they are generating which is converted to speed. Athletes are able to track fitness and compare themselves to other athletes (Geer, 2018). Coaches are able to evaluate the rowers potential to actually move the boat on the water. However, gathering data on technique, using only the ergometer, is limited. Timing can only be gauged based on strokes per minute, displayed on the monitor, and technique can be partially shown using the force curve that the monitor on the erg displays live during a stroke. The force curve is able to show the total force that is created with the legs, back, and arms during each stroke (Breiland, 2017).

While this metric is helpful, there is no current display that breaks the stroke down into its key elements individually: leg drive, back swing, and arm pull. Since there is no current technology on the market there are no engineering standards that exist for the product. Accurately displaying relative positions and timing of these elements will allow athletes to make minor adjustments in timing of each element of the stroke and ultimately the athlete will be able to improve technique. This will also serve as a useful tool to coaches trying to analyze the athlete's stroke.

In order to achieve our final design, our team had three design iterations. The first iteration of the project was completed using the motion capture facility in PracticePoint. The test subject was outfitted with reflective markers on the anatomical landmarks and a Delsys IMU sensor in the center of the back. Two Delsys IMU sensors were also fixed to the seat and handle of the erg. Acceleration data of the seat, handle, and back was collected from the IMU sensors. Position data was collected using the Vicon motion capture system and the reflective markers on the test subject. The primary conceptual design was the visualization that was created from this data. Matlab was used to visualize acceleration over time and the position over time. This iteration makes obvious that it is possible to isolate the acceleration of the three parts of the stroke using three sensors located on the seat, back, and handle. In the second iteration, an instrumented system was developed to break down the elements of the stroke in real time. MEMS sensors were placed in the same locations. Sensor data was collected by a Raspberry Pi as the test subject was rowing on the erg. These values were displayed while they were rowing. They were able to see distinct differences between consecutive strokes. In the final design, the model was applied to the data. This yields the independent acceleration values of each element. Unique colors were assigned to each element for easy identification across charts and for easy identification of back usage. Hopefully this will help to investigate the association between excessive back usage effect and injury. The display updates after every stroke, giving them adequate time to interpret. It also allows them to compare consecutive strokes easily.

Our team also had a few different iterations for the visualization of the data being collected. The early visuals made from motion capture systems in PracticePoint gave helpful insight to the specifics of the stroke. While the graphs that were produced from the sessions and had a different visualization method, it still provided accurate information for timing and position of the stroke.The later visuals made using a real time display gave further, more specific insight into the stroke. Between just the few test subjects, it seems that the stroke can be broken down into three parts. Each acts in consequence of the former. How the elements behave in higher level athletes is to be determined.

Acknowledgements

The team would like to thank our Professors Tiffiny Butler, Lane Harrison, and Selcuk Guceri for the guidance they have provided over the course of the year. The team would also like to thank our sponsor Jon Rourke, who formulated this project. In addition the team would like to thank Chris Nynz for the help that was provided in PracticePoint.

Authorship

Section	**Writer**	**Editor**
Abstract	Josephine Bowen, Blake Dobay, Ben Thornton, Marc Reardon	All
Executive Summary	Josephine Bowen, Marc Reardon	All
Ch. 1: Introduction	Josephine Bowen	All
Ch. 2.1: The sport of rowing	Marc Reardon	All
Ch. 2.2: Introduction to biomechanics	Ben Thornton, Josephine Bowen	All
Ch. 2.3: Common Injuries in Rowing	Ben Thornton, Josephine Bowen	All
2.4: Current Tools used to Visualize the Stroke	Blake Dobay, Marc Reardon	All
Ch. 2.5: Sensor Implementation	Blake Dobay, Marc Reardon	All
Ch. 3.1: Biomechanics Methodology	Ben Thornton, Josephine Bowen	All
Ch. 3.2: Computer Science Methodology	Blake Dobay, Marc Reardon	All
Ch. 4.1: Initial Client Statement	Blake Dobay	All
Ch. 4.2: Revised Client Statement	Blake Dobay	All
Ch. 4.3: Objectives	Blake Dobay	All
Ch. 4.4: Needs Analysis	Josephine Bowen	All
Ch. 4.5: Primary Conceptual Design	Ben Thornton, Josephine Bowen	All

Ch. 4.6: Alternative Conceptual Designs	Blake Dobay, Marc Reardon	All
Ch. 4.7: Final Design Selection	Marc Reardon	All
Ch. 5.1: Testing Procedures	Marc Reardon	All
Ch. 6.1: Experimental Methods	Ben Thornton	All
Ch. 6.2: Data Analysis Final Product	Josephine Bowen	All
Ch. 6.4: Data Analysis Biomechanics	Josephine Bowen, Ben Thornton	All
Ch. 6.5: Product Impacts	Josephine Bowen	All
Ch. 7.1: Product Feasibility	Marc Reardon	All
Ch. 7.2: Design Limitations	Blake Dobay, Marc Reardon	All
Ch. 8.1: Conclusions	Blake Dobay, Marc Reardon	All
Ch. 8.2: Recommendations	Blake Dobay, Marc Reardon	All

Chapter 1: Introduction

Rowing is a physically and technically demanding sport that requires all muscle groups in the body to work in a coordinated sequence to create a powerful and efficient stroke. An effective stroke will be the results of proper timing, technique and power application.

The ergometer has become one of the most useful tools for the general rower, it allows an athlete to receive live feedback on speed, power application, and stroke rate over time. This allows experienced athletes to gather data related to the power they are generating which is converted to speed. It can also help coaches to evaluate the rowers potential of actually moving the boat on the water. Therefore if the rower is also able to develop the correct technique on the erg then this is less the rower needs to learn when they are actually in a boat on the water. For our project our team will focus on improving the technique of the rower on the erg so that they can easily apply the same technique when they are on the water. However, gathering data on technique using only the ergometer is currently limited. Timing can only be gauged based on strokes per minute, displayed on the monitor, and technique can be partially shown using the force curve that the monitor on the erg displays live during a stroke. While these metrics are helpful, there is no current display that breaks the stroke down into its key elements: leg drive, back swing, and arm pull. Accurately displaying relative positions and timing of these elements will allow athletes to make minor adjustments in timing of each element of the stroke and serve as a useful tool to coaches trying to analyze their athletes stroke.

The biomechanics of the rowing stroke has been studied for over 50 years in the rowing community (Baca, 2019). Optimal stroke technique has yet to be proven, and every coach has a different preference when it comes to technique and style of execution. Like other sports, technique has a lot to do with the coaching involved. There are many coaching tools on the market that attempt to facilitate the teaching of the stroke, but none that enable the coach to visualize each element of the stroke independently. Using 3-D motion capture hardware and software will allow the stroke to be quantitatively visualized, therefore making more accurate estimates as to what needs to be changed during the stroke.

The goal of this project is to expand on the practicality of the ergometer by developing a visualization tool that displays data from body positions throughout the stroke. This tool will allow for more intuitive and effective training while using an ergometer. Currently, there is none widely available that is easy to use. This device will be a useful coaching tool that provides detailed feedback to the rower as they row.

Chapter 2: Literature Review

2.1 The sport of rowing

Rowing competitions are not like other competitions in sports. There are no national sporting leagues for rowing, but there are teams. Rowing teams are called crews, and each crew is either out of a university, boat club, or a whole country. Boat clubs that are geographically close to each other typically have competed for generations. Rowing competitions are more traditional in this way, but in this age there are more invitational events that hundreds or even thousands of crews race at, like the Head of the Charles in Boston, MA. Races can even have dozens of crews competing at the same time: rowing down the same river in single file. Races have never had a universally required distance. The distance of the race usually comes down to the distance of open water available for racing. However, in the Olympic events, there is a standard distance of 2000 meters that the athletes compete and train for ("Rowing Basics", n.d). For the most part, the race courses are straight as possible and the boats race side by side to the finish line. The other kind of racing, done in single file, is called head racing and is typically done when the course is curvy.

The boats used for rowing are called racing shells. Rowers sit on a seat that slides back and forth on a track in the shell and their feet are strapped into the boat in front of them. The oars are held in place by a rigger, which helps leverage the oar in the water ("Rowing Basics", n.d). The rowers hold the oar with both hands and press their feet against the foot-plates to pry the boat through the water towards their backs. Figure 1 shows a classic racing shell designed for 8 rowers.

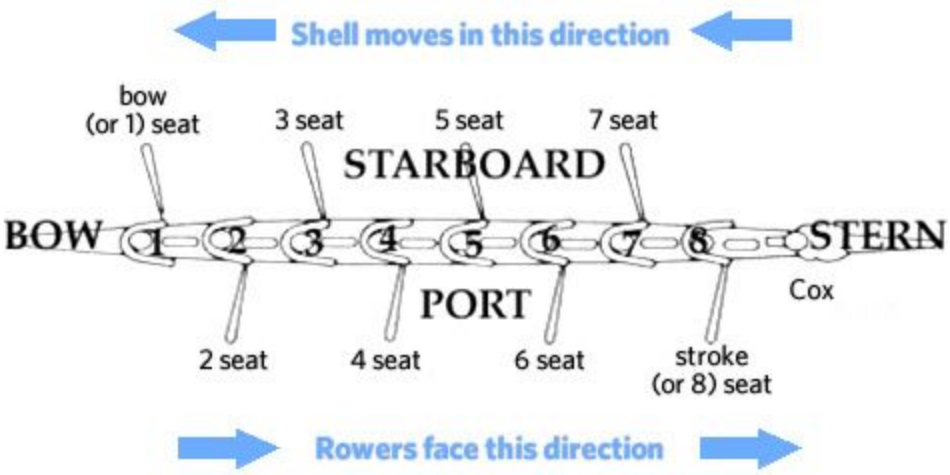

Figure 1. Standard 8-man rowing shell straight-rigged (Whitman, n.d.).

There are several different competitive boat types to date. The most popular boat type by far is the eight man boat called an eight seen in figure 2. At the most elite level, crews desire to win competitions in the eight more than other boat types.

Figure 2. Polish eight racing on a buoyed course ("Empacher Racing Eight", n.d.).

The other types of boats work in the same way, but are designed for less rowers. There is a four man boat called a four or a quad (depending on whether it's designed for sweeping or sculling, respectively), and two man boats called a pair or a double. The sweeping boats are made so that each rower uses one oar on one side of the boat. The sculling boats are made so that each rower uses two oars with one on each side of the boat ("Rowing Basics", n.d). The common boat types used in competition can be seen in figure 3 below.

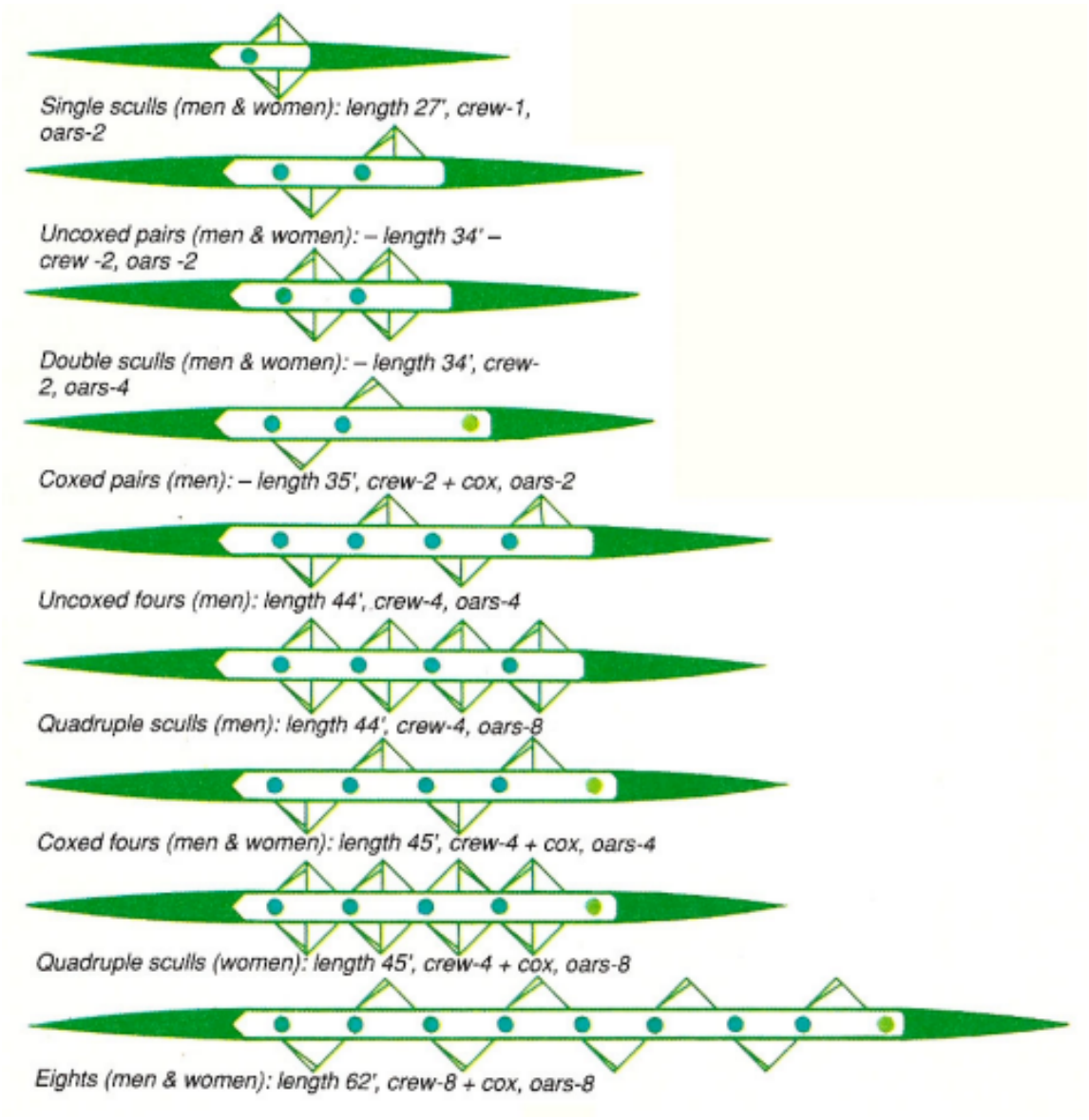

Figure 3. Different types of boats used in competition (Malacrida, 2020).

There are also different kinds of oar shapes that are popular with rowers of all levels. The main kind of oars are the rectangular edged blades shown in the image of the Polish eight ("Empacher Racing Eight", n.d.). There are other kinds of oars that have different edge types that are permitted for use in rowing competitions, but the rectangular blades are currently the most popular. The type of blade that the crew uses comes down to coaching preference.

Crews usually have their own style of rowing, which is usually a product of coaching. There are more traditional ways of rowing and there are also more contemporary ways of rowing. Coaching has evolved, and it continues to evolve with the introduction of new technology. This happens relatively slowly with rowing however, because it is and has always been a traditional sport. Yet there remains a variety of rowing styles between crews. The

interesting part is that almost every style on the spectrum has been successful. It is very difficult to identify a particular style as being more effective. This project attempts to dissect some of this mystery, but culturally there is not a best style. Universities, boat clubs, and countries all have identifiable styles that are unique to their crew. The specific differences in style come down to the timing of the legs, trunk, and arms, in that order. The timing of these elements have been contemplated by every coach molding his/her rowers.

2.1.1 Basics and Anatomy of the rowing stroke

The rowing stroke is a complex motion that engages almost all muscle groups in the body. Many people think of rowing as an upper body sport when really the majority of the power comes from the rowers legs (US Rowing, 2019). The rowing stroke is comprised of four parts: the catch, the drive, the finish and the recovery. At the catch, the tibia is completely vertical the femur is approximately 30 degrees distal to the tibia. The torso is angled towards the femur, and the arms are fully extended so that there is no bend at the elbows. The next phase is the drive where the athlete engages their abdominal muscles and applies pressure to the footboards. As the athlete puts pressure against the footboards the legs start to fully extend until the knee reaches an angle of approximately 180 degrees. The rower also engages the arms pulling the handle towards the torso and bending the elbows. After completing the drive the rower is at the finish position. At the finish the legs are fully extended, the handle is against the upper abdominal muscles, the shoulders are engaged, the abdominal muscles are engaged and the upper body is at a 10 to 15 degree angle posterior to the pelvis. The next position is the recovery, which is comprised of the movement that allows the rower to move back to the catch position. During the recovery the order of movement of the body parts is very important. First, the hands move away from the body in a horizontal line towards the catch. The body then follows the movement of the hands rotating to a 20 to 30 degree angle anterior to the pelvis. Once the body reaches this angle the seat starts to move forward as the rower draws themselves up towards the catch. The knees come up until the rower is back in the catch position, described earlier, with their forward body angle and shins in a vertical position (US Rowing, 2019). You can see the four parts of the rowing stroke and the muscles that are activated during each phase in the figure 4 below.

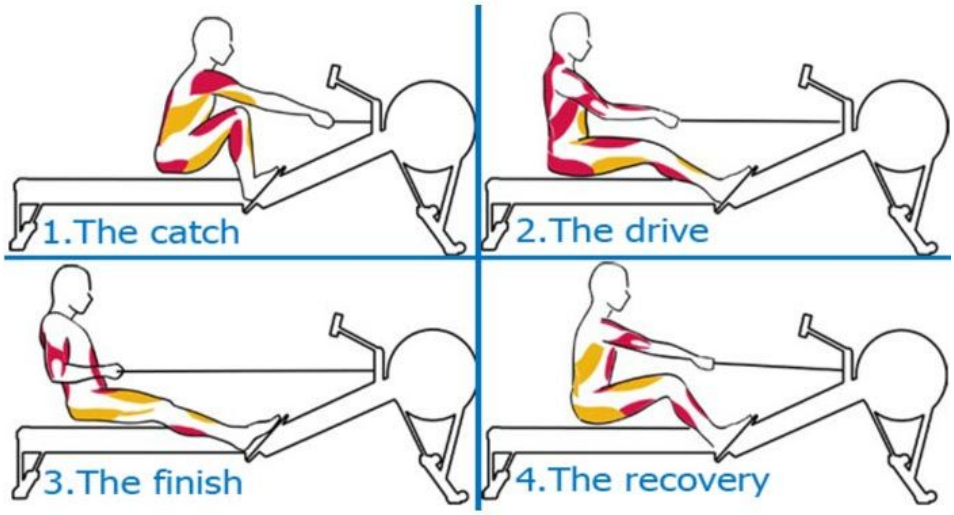

Figure 4. The four phases of the rowing stroke (US Rowing, 2019).

In all forms of rowing these four different phases apply and are sequenced in the same order. However, when it comes to technique there are multiple styles each with their own slight deviations that are followed. According to Klesnev there are four extreme styles (Kleshnev, 2016). Most rowers do not row with just one style but with a combination of them. In the book *The Biomechanics of Rowing* Kleshnev refers to the four styles as Adam, DDR, Rosenburg, and Grinko. These four styles can be seen in figure 5 below.

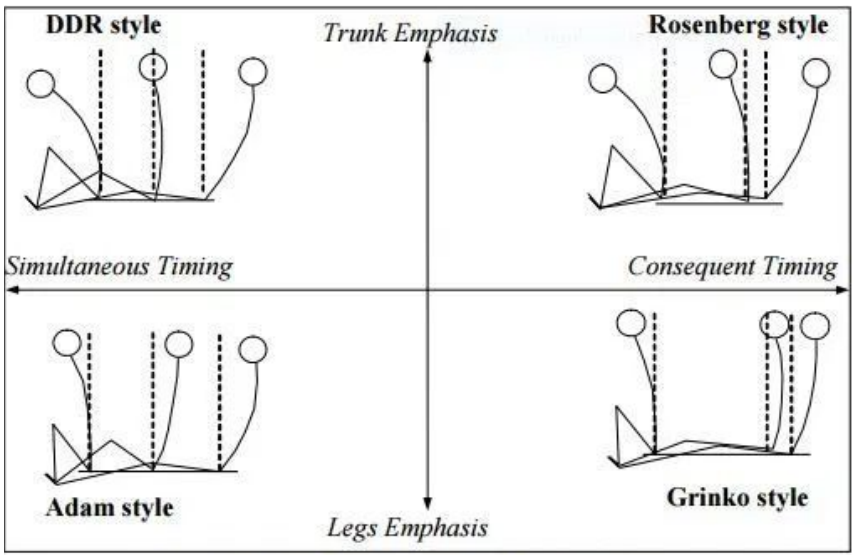

Figure 5. The four rowing styles (Klesnev, 2016).

In 1977 Klavora defined the first three rowing styles: DDR, Rosenberg, and Adams. These styles were created based on the movement of the legs and trunk. In the diagram above the x-axis represents the timing sequence of the legs and trunk in relation to each other and the y-axis represents which segment is emphasized. The DDR style is defined as a stroke where the drive begins with a large, forward declination of the trunk. This movement is then followed by a simultaneous movement of the legs. The Rosenberg style starts the same as the DDR style with a large, forward declination of the trunk. Following this the legs then engage, unlike the DDR style the legs extend without movement of the trunk. After the legs extend the trunk moves into a layback position. The Adam style is similar to the DDR style where the legs and trunk move simultaneously. However, unlike the DDR style the Adam's style has a long leg drive and less forward declination of the trunk (Klesnev, 2016).

However, these three strokes do not complete the above figure, there is still one style that is missing. The stroke that is missing is one that emphasizes the leg movement but also has simultaneous timing. This style was named Grinko after the Russian coach Igor Grinko. It took coaches years to understand how this style of rowing could be beneficial but Igor Grinko continued to coach this style. Igor Grinko went on to coach many rowers who became world champions and even olympic medalists. Once coaches saw this and started to understand this style better they tried to incorporate it into their own teachings (Klesnev, 2016).

Researchers analyzed the power curve that could be created from each of these styles. They were able to determine that a stroke that consists of simultaneous movement of the legs and trunk will create a rectangular shaped curve but show less peak power. In the styles where the legs and trunk move sequentially the curve is more triangular and has a higher peak force (Klesnev, 2016). This shows that overall the rower is able to generate more power when they move their legs followed by their back rather than moving the two simultaneously. Power curves for each body segment as well as full body motion can be seen in figure 6 below.

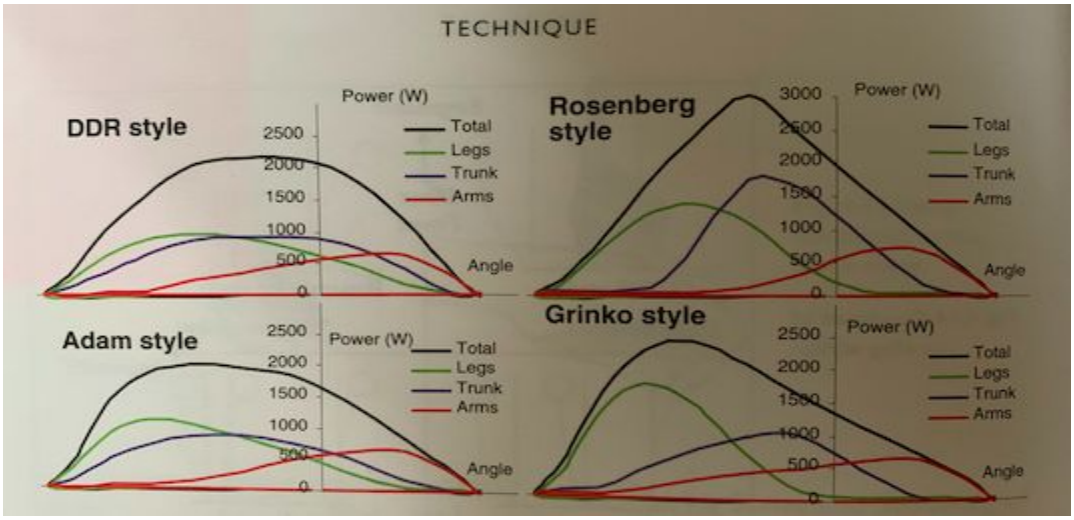

Figure 6. Power curves of the four rowing styles (Klesnev, 2016).

Due to the difference in rowing styles it is hard to define what the “perfect” stroke is. However, it is important to have a picture of the ideal stroke in mind. If the rower can picture what the ideal stroke is then they can aspire to row like that. If they have no aspiration then they have no way of knowing if they are getting better or worse. Having the aspiration also helps the rower to avoid techniques and bad habits that could cause injury. The ideal stroke will be different based on the rowers size and shape but can be determined by biomechanics (Breiland, 2018).

No matter the size and shape of the rower, the same sequence during the stroke is used. During the catch the arms are straight, the head is still, and the shoulders are level. The torso has a slight anterior lean that is initiated from the hips to allow the shoulders to remain anterior to the hips. The shins of the rower are in a vertical position. The catch position can be seen in figure 7 below.

Figure 7. The catch (“Muscles used”, 2019).

From the catch the rower then proceeds into the movement of the drive. During the drive the legs are activated first, the back then swings past the vertical position and then the rower pulls on the handle with the arms. During this motion the hands should remain on a level plain creating a straight line from the flywheel to the body of the rower. Once this sequence is completed the rower should be at the finish. In this position the torso is in a slight layback position, posterior to the hips and the core of the rower is engaged showing that the rower is in a position of power. The legs are fully extended and the handle is held slightly inferior to the ribs. In this position the shoulders and arms are relaxed and wrists are flat and not in a cocked position. The finish position can be seen in figure 8 below.

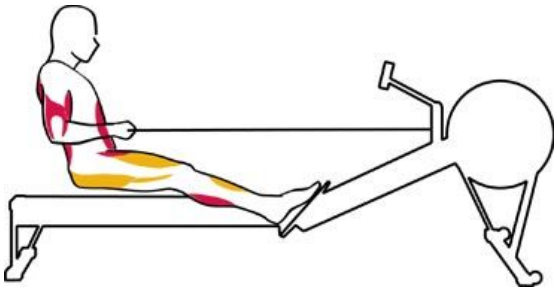

Figure 8. The finish (“Muscles used”, 2019).

After arriving at the finish the rower goes into the recovery phase to get back to the catch. During the recovery the arms are extended first and then once the arms are extended the torso follows, creating a bending motion from the hip. After the hands pass over the knees the legs start to bend and the seat is gradually moved towards the flywheel. Once the rower reaches the catch position they are able to start this sequence again (Cheri, 2019).

2.1.2 Rowing on the Ergometer vs. The Water

There are three types of rowing: sweeping, sculling, and ergometer (erg) rowing. In sweeping the rower is driving a singular blade on one side of the boat (either port or starboard). In sculling, the rower is driving two smaller blades, one on each side of the boat. In ergometer rowing, the rower is on a machine that simulates the technique with a symmetrical handle rather than an oar. Minus the hand skills involved in each type of rowing the technique used, specifically the timing of each segment remains the same.

The erg is an exercise machine that was developed by Dick and Peter Dreissigacker as a way to both simulate the rowing stroke as well as provide comparable data to the work being done when rowing on the water. Since the first erg was developed in 1981 there have been substantial improvements made (Geer, 2018). In figure 9 there is an image of the first erg and in figure 10 there is an image of what the erg looks like today.

Figure 9. Model A, the first ergometer (Geer, 2018).

Figure 10. A model of the current ergometer (Geer, 2018).

Although the primary techniques used on the water and on the erg are similar there are still many differences between rowing on the water and rowing on the erg. There is a significant difference between the handle velocity and shell acceleration on the erg vs. rowing on the water therefore the erg should only be used for cross-training and cannot completely replace on water rowing. One of the main differences between rowing on the erg and rowing on the water is that on the erg the footplate is stationary which increases the inertial forces. Another major difference is that on the water the acceleration of the boat has a big effect on the rowers performance, where that can not be simulated on the erg. On the water the handle force and leg speed increases faster than on the erg. This is due to the fact that on the erg the rower is interacting with a stationary support where on the water the rower is interacting with a mobile point of support. There is also a difference in the gearing ratio in the boat vs. the erg which also affects the magnitude of the handle force (Kleshnev, 2005). The difference in the gearing ratio can be seen in figure 11 below.

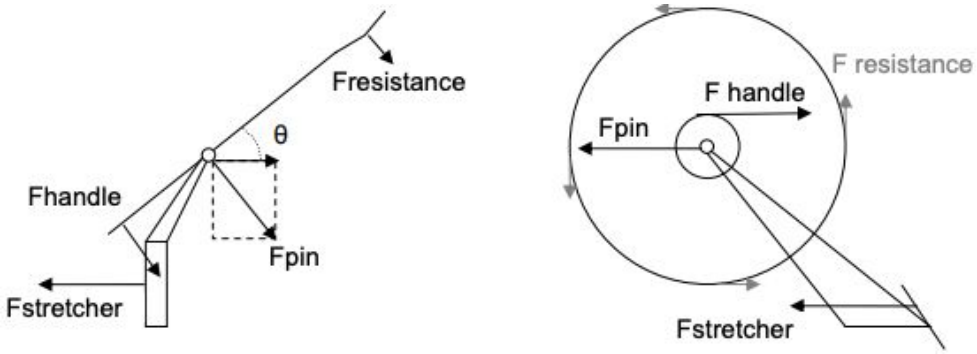

Figure 11. Gearing ratio in the boat (left) and on the erg (right) (Kleshnev, 2005).

The difference in the handle force and speed on the water vs. on the erg can be seen in the graphs below in figure 12.

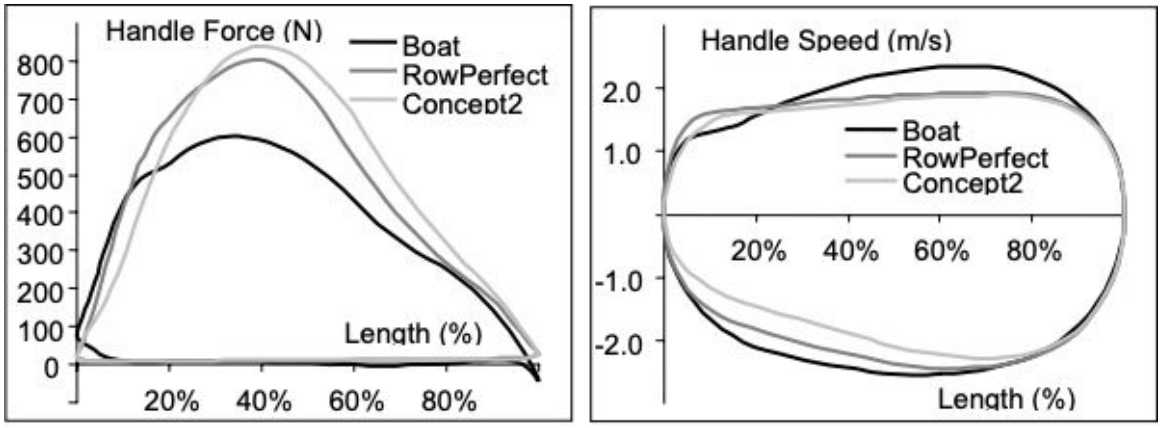

Figure 12. Graphs of the handle force and speed during both scenarios (Kleshnev, 2005).

Rowing on the erg versus on the water is visually the same and incorporates the same timing ratios of body segments; however, as shown above, there are significant differences in mechanics. A table of the similarities and differences between on water rowing and ergometer rowing can be seen below.

Table 1. Similarities and differences between water and ergometer rowing.

Similarities	Differences
● Major techniques ● Stroke components and motions ● Muscle activation	● Additional technique (ex. blade entry) ● Starboard vs. port ● Handle velocity ● Shell acceleration ● Gearing ratio

2.2 Introduction to biomechanics

The biomechanics of the rowing stroke can be broken down as the heart of the sport. The stroke can be broken down into quantitative data that relates to the physical motion that the athlete is doing. A way to analyze complex motionsis through motion capture. For the purpose of the rowing stroke, two dimensional and three dimensional motion capture will be used in the data collection. Two dimensional motion capture will be in the form of a video, and three dimensional motion capture will be through the Vicon motion capture system. Both will assist in relating data to a physical position and timing of the stroke. Essentially, the motion capture data will be used to determine body angles, forces, and moments at specific joints, along with the relative timing. Reflective markers will be placed across the body in order to create a full 3D digital model of the rowing stroke. The markers will be placed in a pattern so that the software can connect all of the markers to create a geometric model of the person including all the joints. The placement of the sensors can be seen in figures 13 and 14 below.

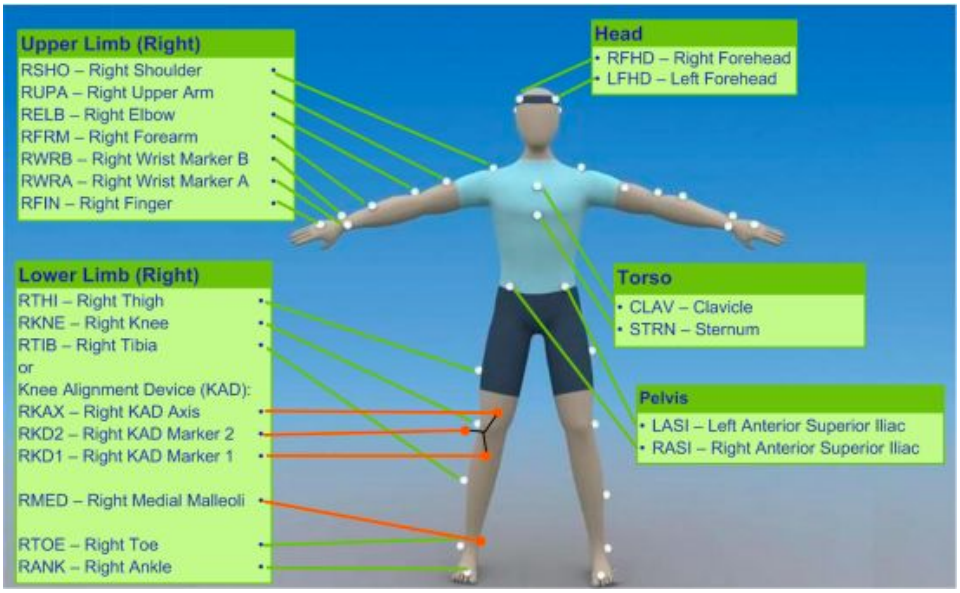

Figure 13. Front view of the anatomical markers placed on the subjects body (Vicon, 2016).

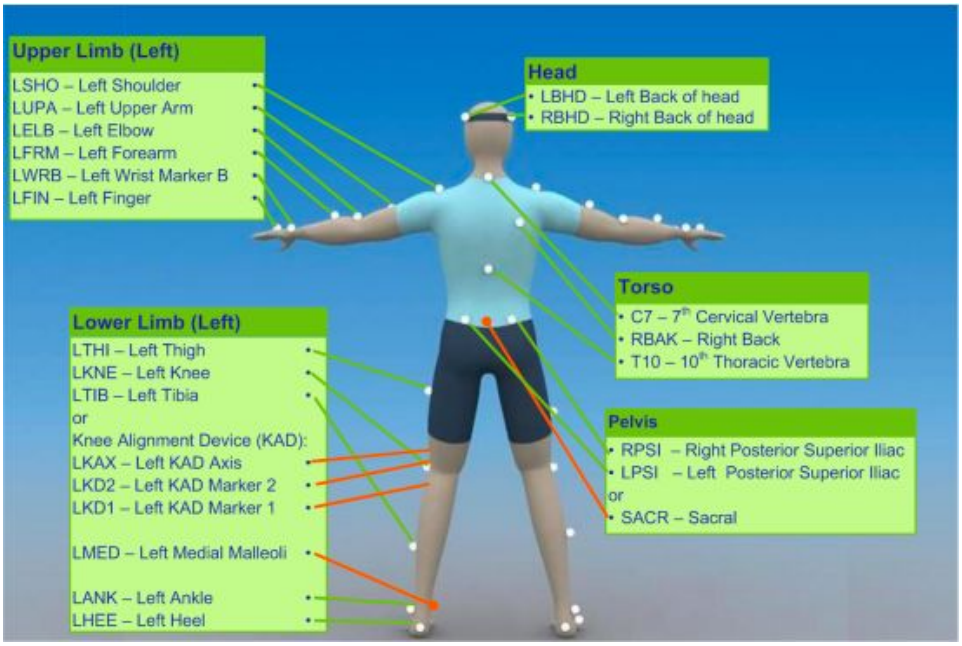

Figure 14. Rear view of the anatomical markers placed on the subjects body (Vicon, 2016).

In addition to the Vicon motion capture system our team will be using Delsys Trigno sensors to collect acceleration data during each part of the stroke. The Delsys Trigno Avanti Sensors are the main tool that will be used for the data collection of the rowing stroke. A sensor will be placed on the seat, handle, and body of the rower so that the data from each section of the stroke can be distinguished.

In addition to measuring the acceleration of the rower the Delsys sensors will also be used to measure muscle activation. This will be done using the electromyography (EMG)

component of the sensor. Sensors will be placed on the calves, quads, fore-arms, triceps, hips, and shoulders. This will allow us to gather enough data to accurately create a musculo-skeletal model to calculate joint loads. While the stroke on the erg is mostly symmetrical on both sides of the body, having three dimensional sensors will allow the team to determine if there are any deviations in symmetry. This will allow us to determine if the body is ever in a position that will compromise the physical health of the rower.

2.2.1 The Math Behind Vicon Motion Capture

The Vicon motion capture system uses a software called Nexus to perform all of its calculations. The user inputs the segment lengths of the test subject along with the test subjects weight. Vicon then uses the segmentation method to calculate the COM of the rower and then creates a data set of how the COM of the rower changes over time. The diagram used for the segmentation method can be seen in figure 15 below. Table 2 shows the proportions that are used to calculate the center of mass.

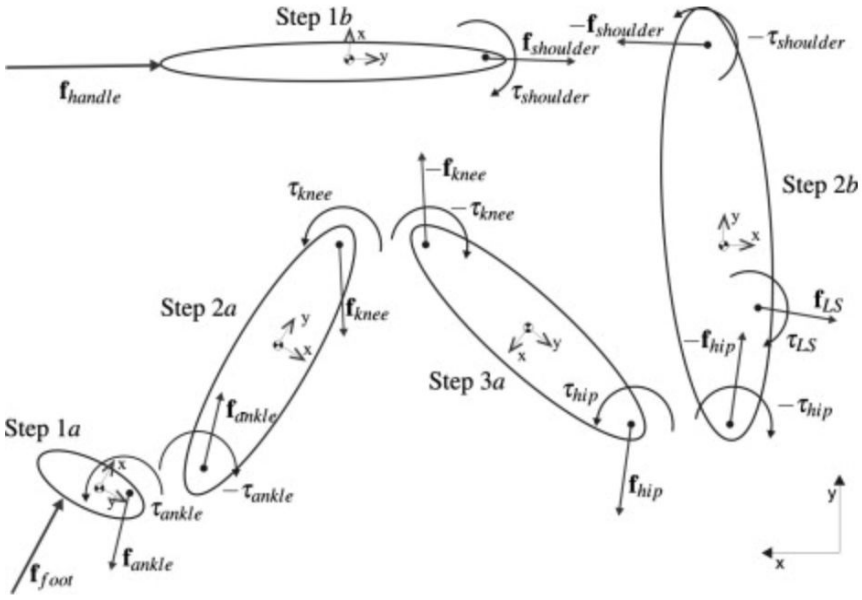

Figure 15. Segmentation of the body (Klesnev, 2016).

Table 2. Segmentation Coefficients from Vicon's Plug-in-Gait ("Vicon Motion Systems", 2016).

Segment	CoM	Mass
Pelvis[a]	0.895	0.142
Femur	0.567	0.1
Tibia	0.567	0.0465
Foot	0.5	0.0145
Humerus	0.564	0.028
Radius	0.57	0.016
Hand[b]	0.6205	0.006
Thorax[c]	0.63	0.355
Head[d]	see below	0.081

The general equations used to calculate the center of mass are:

$$COMx = \frac{m1*x1+m2*x2+m3*x3...}{m1+m2+m3...}$$

$$COMy = \frac{m1*y1+m2*y2+m3*y3...}{m1+m2+m3...}$$

The Vicon software is also able to calculate the angles of each of the joints on the body based on the biomechanical model created of the test subject. The software compares the relative orientations of the segments that are proximal and distal to the joint that is trying to be measured (Vicon, 2016). A data set is then created of the change in angle over time for the duration of the rowing motion. The software is then able to create a graph of position over time that can be used to compare to the acceleration over time.

Although not used for this project, due to the limitations of the size of the force plate, the Vicon software also has the ability to calculate the forces. If the team had collected force data then the team would be able to calculate the moments on the joints. The diagram and equations used for this process can be seen in figures 16 and 17.

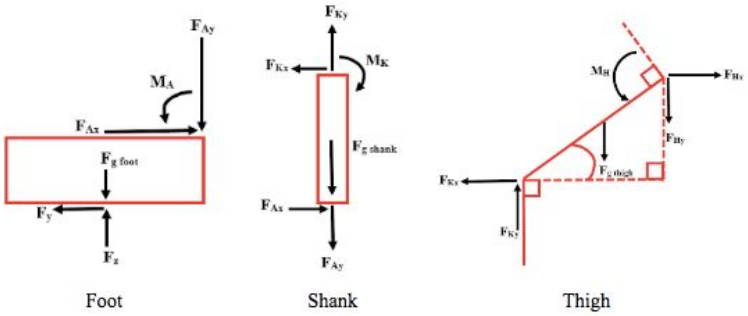

Figure 16. Diagram to show location of forces and moments on the lower body.

$$\sum F_y = F_z - F_{ay} - F_{g\ foot} = 0$$
$$\sum F_x = F_y - F_{ax} = 0$$
$$\sum M_{ankle} = M_{ankle} - F_{g\,foot} * \frac{\iota_{foot}}{2} + Fz * \frac{\iota_{foot}}{2} + F_y * l_{foot} = 0$$
$$\sum F_y = F_{ky} - F_{ay} - F_{g\ shank} = 0$$
$$\sum F_x = F_{ax} - F_{kx} = 0$$
$$\sum M_{knee} = M_{knee} - F_{g\ shank} * \frac{w_{shank}}{2} - F_{ay} * \frac{w_{shank}}{2} + F_{ax} * l_{shank} = 0$$
$$\sum F_y = F_{ky} - F_{hy} - F_{g\ thigh} = 0$$
$$\sum F_x = F_{kx} - F_{hx} = 0$$
$$\sum M_{hip} = M_{hip} - F_{g\ thigh} * l_{thigh} * \frac{cos(\theta_{knee} - 90)}{2} - F_{kx} * l_{thigh} * sin(\theta_{knee} - 90) + F_{ky} * l_{thigh} * cos(\theta_{knee} - 90) = 0$$

Figure 17. Equations to calculate sum of the moments and forces.

2.2.2 Delsys Sensors

Initial data collection for the biomechanics of the rowing stroke will be done with the Delsys Trigno Sensors. These sensors are able to visualize any motion in a confined area. With sixteen sensors, data will be gathered from every joint that is majorly involved in the stroke. This will allow us to accurately determine the timing, muscle activation, and relative position of each joint and the surrounding muscles. Using the sensors, we will collect data that represents the motion of proper rowing, as well as improper rowing. This will give us an idea as to what the data will look like for both cases.

2.3 Common Injuries in Rowing

The most common injuries in rowing come from overuse due to the repetitive nature of rowing. The injuries are related to both the volume of training and the technique used. The most common injuries are to the knees, lumbar spine, and ribs (Hosea, 2012). With other injuries being to the shoulder and wrist. Injuries are then aggravated when rowers try to row through the pain and their other muscles try to compensate for their injury (Parkinson, 2020).

2.3.1 Common Injuries (Upper Body)

The back functions as a cantilever and helps to transfer power between the legs and the oar (the handle in the case of the erg). One common back injury is a lumbar disk injury also known as “slipped disk”. This injury occurs when excessive force is put onto the lumbar spine. The rower pulls the oar/handle backwards while angled forward which puts strain on the back if the rower does not engage the core. Another back injury is an injury to the sacroiliac joint.This is generally caused because of overuse from high volume training. The sacroiliac joint is located in the lower back, one on each side of the spine. The joint acts to connect the spine to the pelvis. This injury is also caused when excessive force is put on the back. Figure 18 below shows the anatomy of a slipped disk injury.

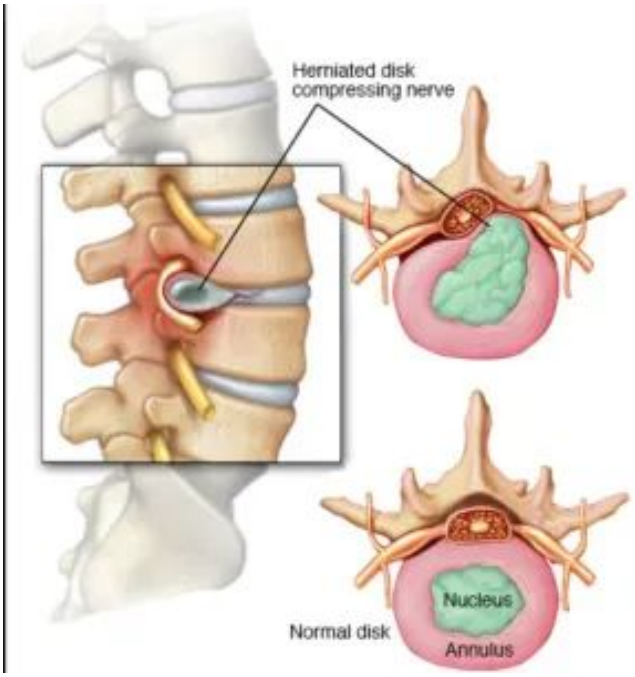

Figure 18. Slipped disk anatomy (“Herniated Disk Treatment”).

Rib stress fractures are another common injury in the sport of rowing. In these injuries it is common to feel the pain in the back and have tenderness over the injured rib. An x-ray image of a rib stress fracture can be seen in figure 19 below.

Figure 19. Rib stress fracture (Hosea, 2012).

Due to the movement of feathering another injury in rowing is wrist injuries. The flipping of the oar perpendicular and parallel to the water is what causes extensor tenosynovitis. The muscles affected by this injury can be seen in figure 20 below.

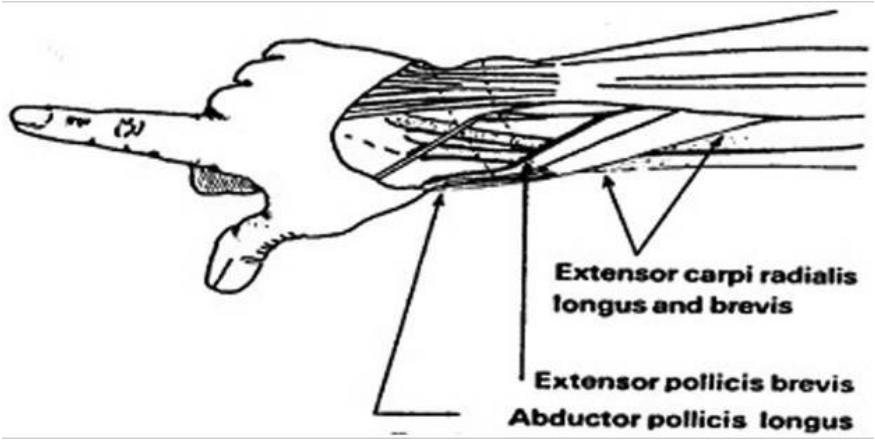

Figure 20. Wrist tendons affected by feathering method in rowing (Hosea, 2012).

2.3.2 Common Injuries (Lower Body)

Another common area for injury in rowing is the knees. There are two common knee injuries: chondromalacia patella and iliotibial band (ITB) friction syndrome. A chondromalacia patella injury results in anterior knee pain during the rowing stroke. Chondromalacia patella can also make it difficult to climb and descend stairs. It also could result in swelling around the knee joint and a clicking noise coming from the knee area during rowing (Hosea, 2012). Injuries to the knees are caused by the repetitive forward and back motion that the knees endure during the

rowing stroke. Proper biomechanics can help combat or attenuate these injuries in rowers. The toes should be lined up with the knees with the foot ties turned slightly outwards. The core muscles should be engaged in order to maintain the correct back posture. The knees should move back and forth in one fluid motion without any jerking. Another way to help prevent this injury is to raise the height of the footstretcher in order to decrease the knee flexion angle at the catch. Figure 21 below shows iliotibial band friction syndrome.

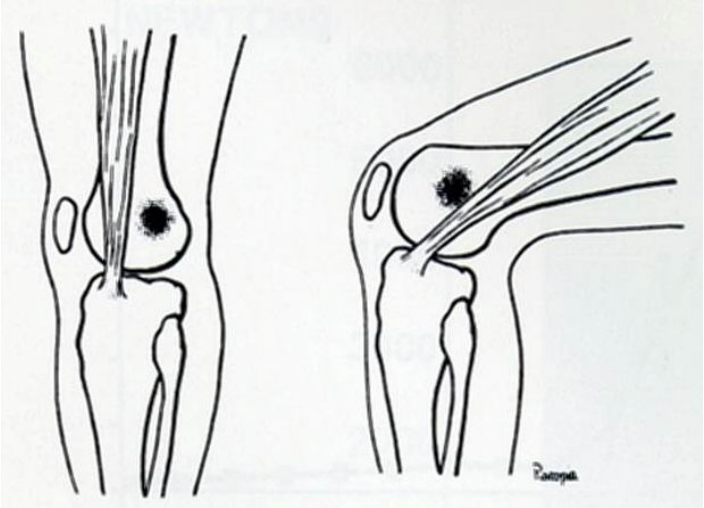

Figure 21. Iliotibial band friction syndrome (Hosea, 2012).

2.3.3 Injury Identification

While the optimal stroke position is up to interpretation of a specific athlete's body type and coach, there are certain techniques and general errors that put the body in a position that creates unnecessary strain. A common injury among rowers can be ribcage stress injuries (RSI). Several published journals have discussed the reasoning behind this and have related that poor stroke mechanics can put the body in a more compromising position than others.(Hosea, 2020) Different stroke/coachings styles will have different tendencies as well. For example, some coaches may suggest the proper stroke is to initiate leg/knee extension from the catch, followed sequentially by the hips and back, while other styles suggest the legs, hips, and back must be synchronously initiated. According to a study (Hosea, 2020), more rowers who practice the latter technique experience RSI more frequently, due to the loading pattern. This is then amplified by the constant loading and unloading nature of the sport. The image below displays the location of RSI in elite rowers overtime. By loading the stroke with both the upper and lower body simultaneously, the torso and rib cage experiences more stress than if they were loaded sequentially. This is also a result of overall bone strength, which can be broken down into bone mineral density and bone structure (Hosea, 2020). The bones of the rib cage do not have the same structure as the long bones of the legs, making them less suitable to be repeatedly loaded

and unloaded. Current studies are being done as to what are the most effective ways to prevent such injuries, while still performing at a high level.

2.3.4 Injury Prevention

Prevention of these injuries can come in several forms. Several published journals have suggested that both mechanics as well as nutrition can contribute to the prevention of rowing related injuries. Several studies have shown that athletes who are consistently rowing at high volumes, such as elite athletes during winter training.

Proper stroke timing and mechanics are key to injury prevention. Many common stroke mistakes can lead to future injuries that can be avoided if they are identified and corrected. One extremely noticeable mistake in rowing is referred to commonly as “lunging at the catch.” Ideally during a stroke, the catch is when the knees are fully compressed, the back is in a position of power, and is not in a slouched state. The general mechanics of this error involve motion of the upper body, after the knees are fully compressed. This generally causes the rowing to over compress, and put back in a position that is more likely for injury. When a rower initiates the stroke, it should be done with the legs and transferred through the abdomen, while the arms remain fully extended. Bending the elbows too early in the stroke can result in tendonitis in the forearm and wrist. On an acceleration graph, this would be displayed as additional positive acceleration with the hands after the catch. This is an extremely common injury among rowers, using a device such as this could potentially inform the athlete of their error and the athlete could make adjustments based on the graphs. Another common mistake in the stroke commonly referred to as “shooting the slide.” This is when the rower engages the legs at the catch of the stroke, but does not engage the abdomen, essentially moving the seat without moving the handle or the flywheel. This difference can also be noticeable in a graph of the seat acceleration. Therefore if there is a tool that can display the change in acceleration of the different components of the stroke it could ultimately help prevent injuries.

2.4 Current Tools used to Visualize the Stroke

At the most elite level, coaches are always searching for marginal gains in the form of seconds. There have been numerous attempts to visualize the rowing stroke with both static graphs from collected data and real-time visuals that are graphed on a per-stroke basis; used to make minute corrections based on the data. One analysis was conducted by The University of Twente in The Netherlands that attempted to utilize machine learning techniques to separate good rowing from bad rowing. They were unable to find bad rowing with absolute posture angles, however, they were able to pick out bad rowing by assessing the variation in the posture angles between strokes in which bad rowers typically were more inconsistent (Bosch, 2015). At the elite level posture angles vary slightly between different athletes because of different technique and body styles of each athlete. These differences make it hard to determine an optimal posture angle for all athletes. However, graphing continuously shows a noticeable

difference between techniques. Even the slightest differences in techniques shows up when using numerical data. Figure 22 graphs posture angle over time for three different sensors. These differences can be reviewed and considered by coaches. Also, key points like maxima and minima can be compared. These differences can then be assessed comparing the visualized data to quantitative differences in the speed of the rower.

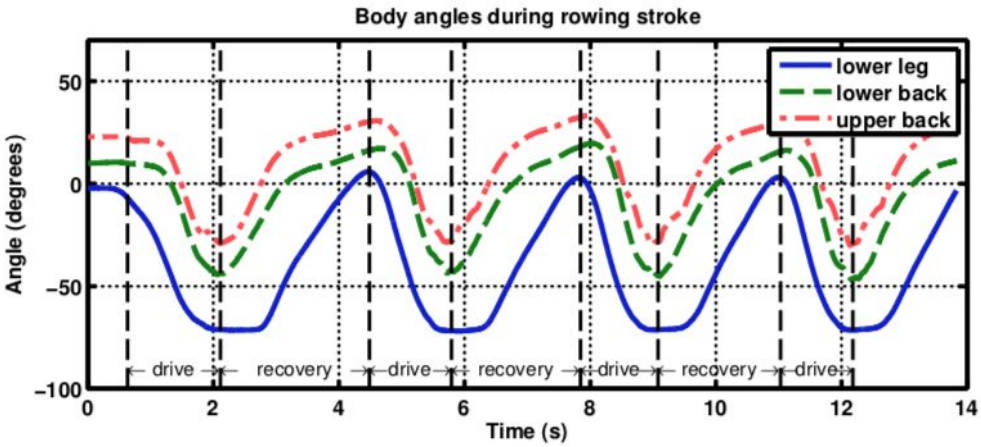

Figure 22. Body angles during rowing stroke (Bosch, 2015).

The BioRowTech System by BioRow is one product that displays data similar to the goals of this project (Figure 23). They display the velocities of the legs, trunk and hands all independently. The handle velocity is a sum of the other three segment's velocities. Our team plans to use the idea that the handle velocity is the sum of the other segment's velocities, and extract the velocities in the same way. When the legs sensor moves, every other sensor moves the same amount. When the back sensor moves, the handle sensor moves the same amount. And when the handle sensor moves alone, it is the only sensor moving. The velocity points on the graph are calculated using these rules. When they take the velocity from the back sensor, they subtract out the legs velocity to get the independent back velocity. This project will utilize similar techniques.

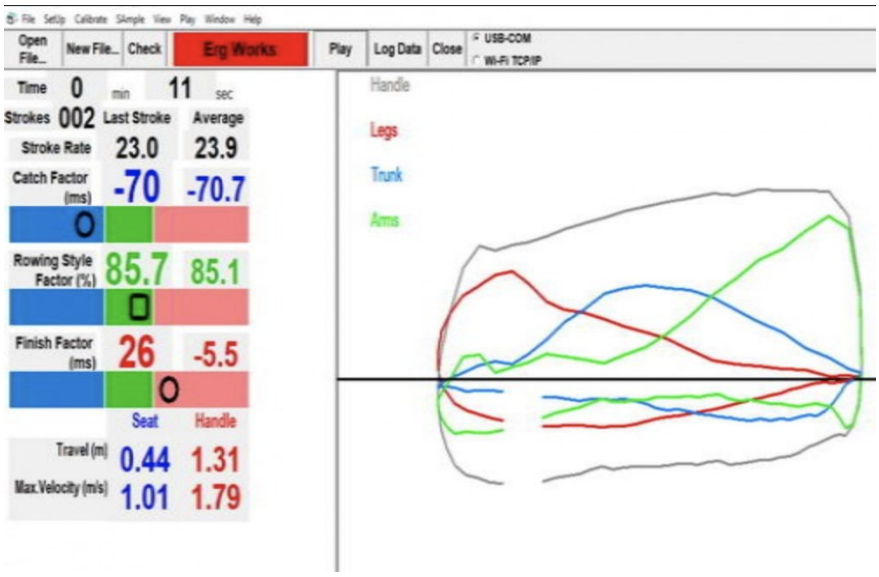

Figure 23. BioRow visualization with three sensors, and a breakdown of the timing elements ("Biorow Systems").

This project aims to create a tool that can assist in the training of rowers, and in doing this the display must be effective at showing the difference between one stroke and the next. Using these line graphs, it is hard to tell how much overlap there is between the curves and where the relative maxima are. It is important that the difference between strokes is easy to see so that when corrections are made they are seen on the display.

The standard rowing machine, Concept2, has a built-in display for showing power output over time. The power at any one moment is a product of the speed of the flywheel, and the rowing machine graphs that value over time for each stroke. Figure 24 shows the rowing machine monitor with the force/time graph displayed.

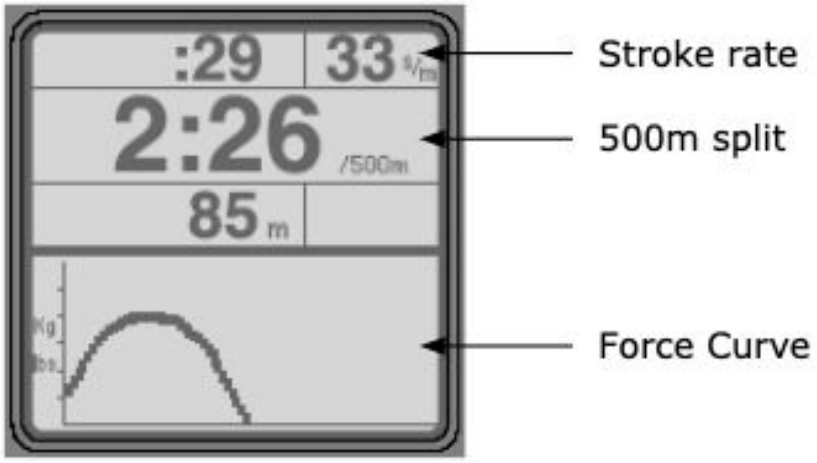

Figure 24. Force curve on a Concept2 ergometer (adapted from "Using the force curve", 2019).

The curve that the display makes is similar to the curve shown on the graphs that were constructed for the Dutch sensor instrumentation project mentioned before. One of the key differences between these two displays for the matter of this project is that the graph in figure 24 is the summation of the force generated by the back, legs and arms, and the graph in figure 23 is broken down into separate elements of the stroke. This project aims to deploy an interpretation of the stroke similar to that of figure 23. To record data for the figure 23 graph, the sensors were placed on the lower leg, upper back, and lower back. For this project, the sensors will be placed in different areas than this, discussed later.

Since the stroke has been envisioned as a curve on the most popular and standardized rowing machine, it might be the easiest understood interpretation of the rowing stroke over time. This project will be focusing on the curve because of its many implications in rowing.

2.5 Sensor implementation

The goal of the application being developed is to provide a visual feedback tool that provides a more complete picture of the stroke. A key challenge in developing this tool is where to position the sensors in a way where the timing of each element can be extracted individually. The Dutch instrumentation project placed the sensors in places that would not enable extraction of each element. Figure 25 shows the sensor placements for the Dutch sensor instrumentation project.

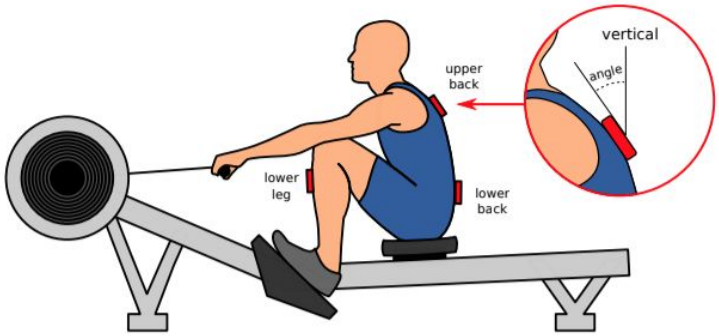

Figure 25. Dutch project sensor placement (Bosch, 2015).

This project aims to extract the distance/time graphs for each of the legs, back and hands. To do this, the sensor must have the capability to measure acceleration, gyroscope, and magnetometer data.The dutch instrumentation project chose to place the sensors on the rowers body this allowed them to extract changing angles over time. Our team has chosen to instead place two of the three sensors on the ergometer instead. Placing the sensor on the ergometer gives the benefits of reduced data noise however only gives acceleration and position data. Showing acceleration and position gives the rower tangible feedback that they can act upon.

Statistics like acceleration are easy for a rower to understand as they can control how fast they execute each part of the stroke.

Three sensors are sufficient to extract the individual timing of each element of the stroke: a single sensor between the shoulders, a single sensor on the handle, and a single sensor on the sliding seat. The seat is one key part of the rowing motion as it moves with the legs of the rower. The acceleration and position of the seat moving towards the catch and through the drive can give information such as the stroke rate, drive time, and drive length. Drive time and drive length are crucial pieces of data as they pertain directly to force applied over the duration of the stroke. Information from the seat movement can also be used when analyzing timing of other elements of the stroke in relation to the movement of the seat. Another key location for the stroke is the torso of the rower. Important data such as body position angle, and timing helps to set up the rowers position at the catch, finish, and body swing throughout the drive. This information can easily be used by a rower to make small changes in positioning that affect his or her stroke. The last important position is the handle of the erg. Position on the vertical axis can indicate the handle height of the rower at the catch, finish, as well as through the drive. Timing of the hands coming out of the finish is also important in setting up the rower's recovery timing. It can also give information on when the hands are moving compared to other parts of the rowers body. Placing sensors on these parts of the rower and machine will give enough information to give a complete visualization of the rowing stroke. To do this, the research was done about visualizing physical movements in other applications.

Chapter 3: Methodology

During the beginning stages of our project our team worked on two main sides of the project: biomechanics and computer science. Therefore the methodology will be split into these two sections accordingly.

3.1 Biomechanics Methodology

3.1.1 Setup

Our team conducted our first data collection session in the PracticePoint facility at gateway. PracticePoint has a motion capture room that is equipped with 10 Vicon Vantage cameras surrounding the perimeter of the room. The first step of the motion capture process is to fit the test subject with reflective markers on the major anatomical landmarks of the individual. Double sided tape was used to attach these markers to the test subject. These markers will be used to create a biomechanical model made up of the major planes and joints. The positioning of the markers on the posterior and anterior of the test subject can be seen in figures 26 and 27 below.

Figure 26. Placement of reflective markers on the anterior of the test subject.

Figure 27. Anatomical markers on the posterior of the test subject.

After outfitting the test subject with the reflective markers a calibration process was then conducted to determine the range of mobility of all the joints of the test subject. The test subject had to conduct a range of mobility movements for both legs, knees, ankles, shoulders, arms, elbows, hips, and neck. This was done by hinging the ankle followed by the knee for both legs. The legs were then swung back and forth in all directions followed by a full rotation of the hips. The elbows were then flexed and extended, the arms were swung in all directions and then the shoulders were rotated. The neck was then rotated in a similar way to the hips. This calibration data was then used to create a scaled biomechanical model of the test subject with accurate joint movements. Three delsys sensors were then added to the system. One on the back of the test subject (sensor 3), one on the handle of the ergometer (sensor 2), and one of the seat of the ergometer (sensor 1). The test subject then sat on the ergometer and rowed without any specified style for two minutes. Then the test subject imitated the four extreme rowing styles: DDR, Adams, Rosenberg, Grinko. The test subject imitated each of these styles for two minutes. Next the test subject imitated two poor rowing techniques, shooting the slide and lunging at the catched. The test subject performed each of these movements for two minutes. Data was then collected from both the vicon system and the delsys sensors for each stroke type. The data collection will be further explained in the following sections.

Three weeks later, another data collection session was conducted at the PracticePoint facility in Gateway. Three weeks gave the group an adequate amount of time to analyze the data from the previous session and determine what changes needed to be made. The team determined that although the data collected was adequate the team also wanted to collect muscle activation data. The team also collected the same data from session one to compare for consistency. The same calibration technique was used and range of mobility tests were completed again. The test subject was first outfitted with the reflective markers as seen in figures 26 and 27. This time six additional Delsys sensors were applied to the body of the test subject. In addition to the sensors on the back, handle, and seat, sensors were added to the right and left quadricep, right and left bicep, and right and left latissimus dorsi. Before these sensors were added the attachment site was cleaned with an alcohol wipe and the dead skin was removed with tape. This was done to improve the EMG connection of the sensor. The sensors were then attached directly to the skin using double sided tape. The EMG capabilities of the sensors were then used to measure the activation of the quadriceps, biceps, and latissimus dorsi. These are the major muscles engaged during the rowing stroke and therefore they were the regions chosen for data collection. Sensor 1 was placed on the seat, sensor 2 on the handle, sensor 3 in the center of the back, sensor 4 on the right bicep, sensor 5 on the left bicep, sensor 6 on the left quad, sensor 7 on the right quad, sensor 8 on the left latissimus dorsi, sensor 9 on the right latissimus dorsi. The test subject then rowed for one minute for each style: Rosenburg, Adams, DDR, Grinko. The test subject then rowed for one minute while imitating lunging and then another minute while imitating shooting the slide. The test subject then rowed as they normally would without trying to imitate any specific style to see how the rowing compared to the specific styles. The team decided to reduce

the time of each rowing style to one minute as that provided a sufficient amount of data for comparison between rowing styles.

About three weeks after the second session, another test session was then conducted with additional sensors added to the test subject. The team decided to measure the muscle activation where injuries commonly occur in addition to the major muscles that are activated during the stroke. The data from the muscle activation from session two was noisy and did not pick up on the majority of the activation. The majority of the displayed movement was residual from the joint movement of the test subject. In addition to all the sensors mentioned in session two, sensors were also added to the right and left flexor carpi radialis and left and right abdominal muscles. These muscles were all chosen due to common injury sites in rowing. The abdominal muscles were chosen due to the fact that a back injury is more likely when the abdominal muscles are not engaged due to more force being applied to the back. For this study sensor 1 was placed on the left bicep, sensor 2 on the right bicep, sensor 3 on the left latissimus dorsi, sensor 4 on the right latissimus dorsi, sensor 5 on the left quadricep, sensor 6 on the right quadricep, sensor 7 on the left flexor carpi radialis, sensor 8 on the right flexor carpi radialis, sensor 9 on the left abdominal muscle, sensor 10 on the right abdominal muscle, sensor 11 on the center of the back, sensor 12 on the seat, and sensor 13 on the handle. Figures 28 and 29 below show the test subject with all the reflective markers in addition to all the sensors (not shown in figure sensors 12 and 13). The data from the muscle activation from session two was noisy and did not pick up on the majority of the activation; the majority of the displayed movement was residual from the joint movement of the test subject. Therefore, for this test session the team tried testing multiple locations for the sensors around the location of each muscle before attaching the sensor to the test subject.

Figure 28. Placement of reflective markers and Delsys sensors on anterior test subject.

Figure 29. Placement of reflective markers and Delsys sensors on posterior of test subject.

3.1.2 Data Collection: Vicon

The Vicon motion capture system proved to be an extremely beneficial tool to our team during the data collection phase of our project. Our team utilized the plug-in-gait software from vicon to measure the complex motions of the rowing stroke. The hardware for this program uses thirty six reflector balls that are placed at crucial locations on the body. The room was set up with infrared cameras that measured the light being reflected off the balls.

Using the Plug-in-Gait software included with Vicon, our group was able to isolate the critical joints involved in the rowing stroke. While Plug-in-Gait is generally used for the intentions of analyzing the walking gait of a desired subject, the same procedure can also be used to gather desirable data for the rowing stroke. Using this tool the team was able to gather data for acceleration and projected moment outputs for each angle of choice. The software was able to compile each of the reflector balls locations on our subject and create a stick figure model shown below in figure 30.

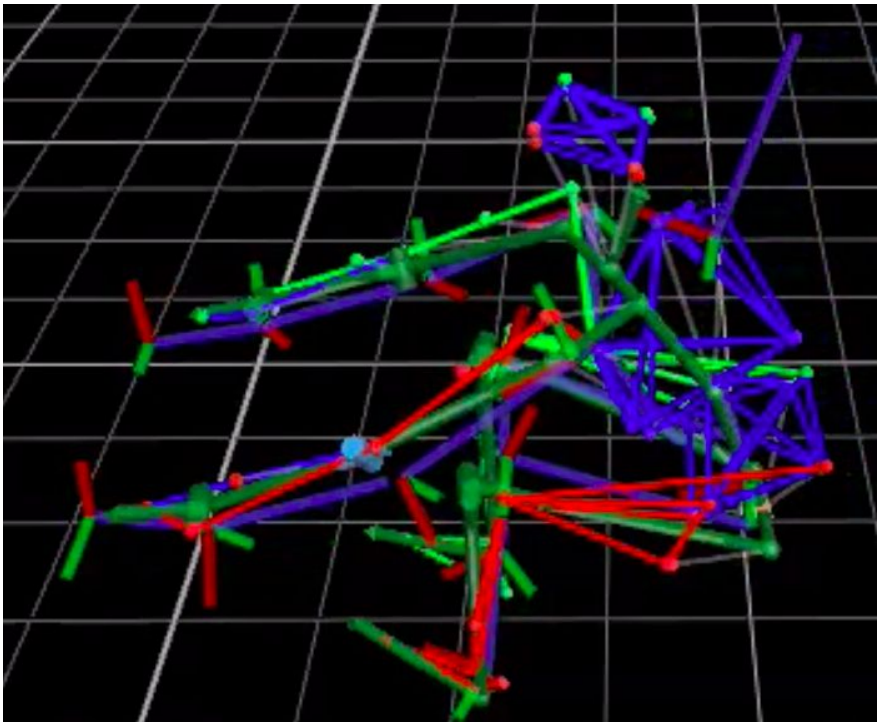

Figure 30. Vicon stick figure of test subject 1 rowing.

From this model and the anatomical dimensions of the test subject that were inputted the software was able to calculate the angles of each of the joints of the model over time. In addition to calculating the angles the software was also able to calculate the change in position of the COM of the test subject in addition to other data points. From all the data collected by the software our team used the plug-in-gait outputs (model outputs) to determine the change in angle

over time for each section of the stroke. The elbow angle was used to identify the timing of the arms. The knee angle was used to determine the timing of the legs. The pelvis angle was then used to identify the change in angle of the back.

3.1.3 Data Collection: Delsys

For the data collection from the Delsys sensors our team collected acceleration data, gyroscope data, and EMG data for each sensor. The data was exported from the software in a CSV file that could be used for analysis. For the first part of the project our team focused mainly on the acceleration data from the sensors. The team focused on the change in acceleration in the primary direction of movement (for this case it was the z-direction based on the orientation of the sensors). The change of acceleration in the x and y directions was minimal and therefore was taken into consideration but not used in data analysis. A range of data equivalent to one stroke was then selected from the data and further analyzed. This process was completed for each of the different stroke types. An explanation of the analysis is described in the following section.

3.1.4 Data Analysis: Matlab

A Matlab program was then created in order to read the CSV files from both the Vicon motion capture system and the Delsys Trigno sensors. This program was created in order to create normalized graphs of that data that can be overlayed on top of each other for comparison. Our team started by creating graphs of the change in knee angle, elbow angle, and pelvis angle over time. The average angle was graphed and then overlaid with a shaded area that showed the standard deviation of the data. The max angle of the knee was used to differentiate between the different strokes so that each stroke could be overlaid on top of eachother. Once the graph was created for all the different angle changes (knee, elbow and pelvis). Another graph was then created for the acceleration of the seat, one for the acceleration of the handle, and one for the acceleration of the back. The x, y, and z acceleration were all plotted on their respective graphs but for the purpose of our project our team will focus on the z acceleration because the acceleration in the x and y directions was minimal. The position graphs were then compared to the acceleration graphs to determine how the change in acceleration related to the change in position of the different joints of the rower. Graphs of the gyroscope and EMG data can also be graphed in the same way in the future. The Matlab script created with the assistance of Christopher Nynz can be found in Appendix C.

3.2 Computer Science Methodology

3.2.1 Data Prototyping

Using Bluetooth enabled MEMS (microelectromechanical system) 9-axis sensors, data can be sent at a high rate around 100 Hz to any Bluetooth enabled device. Our team used a

sensor called the MetaMotionR, shown in figure 31. It is programmable with a proprietary API (application programming interface) which enables our team to interface with the sensor in a number of different ways, including sensor activation, and calibration as well as log and stream data. The data available for use includes 3 dimensional acceleration (g's), 3 dimensional magnetic flux density (microTeslas), and 3 dimensional orientation.

Figure 31. Bluetooth 9-axis sensor developed by MetaMotionR.

The accelerometer records acceleration data in the format shown in figure 32. Since this project aims to extract acceleration in each part of the stroke, this will be the data to work with. However, the other data will be necessary later to help with reducing error.

	A	B	C	D	E	F
1	epoc (ms)	timestamp (-0500)	elapsed (s)	x-axis (g)	y-axis (g)	z-axis (g)
2	1580310547701.00	2020-01-29T10.09.07.701	0	0.001	0.014	0.012
3	1580310547709.00	2020-01-29T10.09.07.709	0.008	-0.028	0.003	0.006
4	1580310547720.00	2020-01-29T10.09.07.720	0.019	-0.035	-0.006	0.014
5	1580310547730.00	2020-01-29T10.09.07.730	0.029	-0.032	-0.006	0.016
6	1580310547740.00	2020-01-29T10.09.07.740	0.039	-0.036	-0.006	0.011
7	1580310547749.00	2020-01-29T10.09.07.749	0.048	-0.033	-0.001	-0.009
8	1580310547759.00	2020-01-29T10.09.07.759	0.058	-0.026	0.008	-0.021
9	1580310547769.00	2020-01-29T10.09.07.769	0.068	-0.016	0.005	-0.018
10	1580310547780.00	2020-01-29T10.09.07.780	0.079	0.001	-0.006	-0.02
11	1580310547790.00	2020-01-29T10.09.07.790	0.089	0.006	-0.015	-0.017
12	1580310547800.00	2020-01-29T10.09.07.800	0.099	0.005	-0.019	-0.027
13	1580310547809.00	2020-01-29T10.09.07.809	0.108	0.001	-0.019	-0.025
14	1580310547819.00	2020-01-29T10.09.07.819	0.118	0.007	-0.031	-0.026
15	1580310547829.00	2020-01-29T10.09.07.829	0.128	0.017	-0.046	-0.02
16	1580310547840.00	2020-01-29T10.09.07.840	0.139	0.018	-0.047	-0.013
17	1580310547850.00	2020-01-29T10.09.07.850	0.149	0.005	-0.04	-0.014
18	1580310547859.00	2020-01-29T10.09.07.859	0.158	-0.006	-0.033	-0.01
19	1580310547869.00	2020-01-29T10.09.07.869	0.168	-0.018	-0.017	-0.006
20	1580310547879.00	2020-01-29T10.09.07.879	0.178	-0.023	-0.009	0.005
21	1580310547890.00	2020-01-29T10.09.07.890	0.189	-0.025	-0.01	0.04
22	1580310547900.00	2020-01-29T10.09.07.900	0.199	-0.034	-0.008	0.031
23	1580310547909.00	2020-01-29T10.09.07.909	0.208	-0.038	-0.008	0.024
24	1580310547919.00	2020-01-29T10.09.07.919	0.218	-0.043	-0.013	0.008
25	1580310547929.00	2020-01-29T10.09.07.929	0.228	-0.038	-0.021	-0.004
26	1580310547939.00	2020-01-29T10.09.07.939	0.238	-0.023	-0.022	-0.009

Figure 32. Acceleration data in units of g's in 3 dimensions, corresponding to time.

Testing for feasibility, our team's sponsor, Jon Rourke, rowed using a MEMS device. One sensor was placed on the slide, and then after rowing for some time it turned out that it is feasible to use them for recording rowing data. The interpolation of the data is consistent, despite a bit of error existing in the raw values. Figure 33 below shows data recorded over a few strokes. Looking at the position curves, there is enough error from integration for the data to drift. Thus, our team cannot use position data. This was an early concern, but later determined not to be because it could be avoided by using only acceleration data.

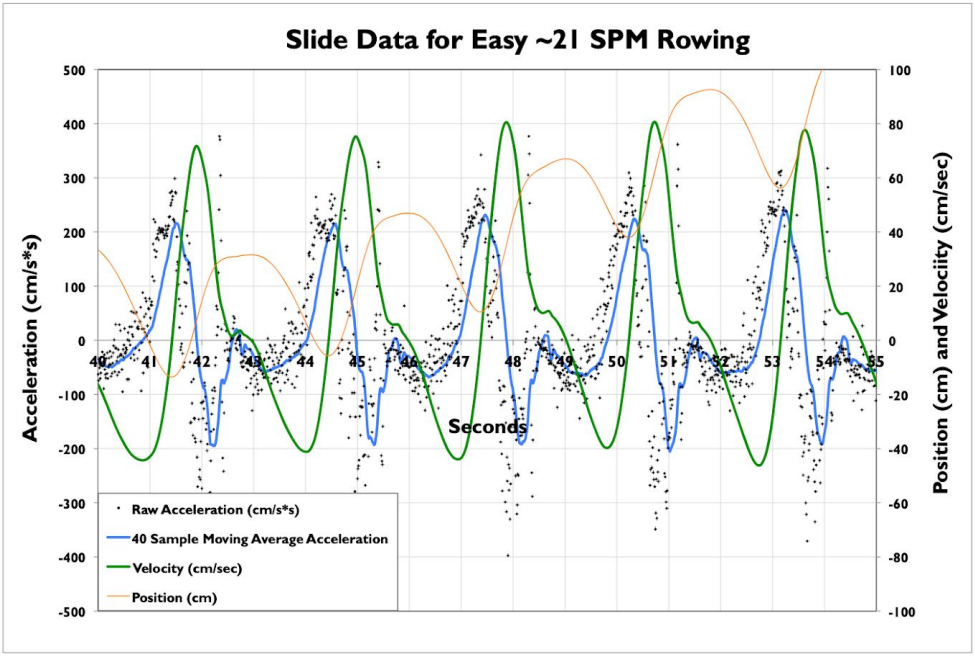

Figure 33. Acceleration data recorded over multiple strokes. Velocity and position obtained by integrating acceleration once and twice, respectively.

Then our team tried all three sensors together. The sensors were placed on the handle of the ergometer, between the shoulder blades of the rower, and on the seat of the ergometer. Sticky tape was used as a temporary fastening technique. Each sensor was placed in the same orientation on the x, y and z planes to ensure that the streamed data from each category was consistent. Whatever axis is parallel to the direction of the drive should be used. In this case, it is the z-axis that is of interest. The sensor placement on the erg and the rower can be seen in the figure below. The three sensors are drawn in blue and are labeled S1, S2, S3. The sensor placement can be seen in figure 34 below.

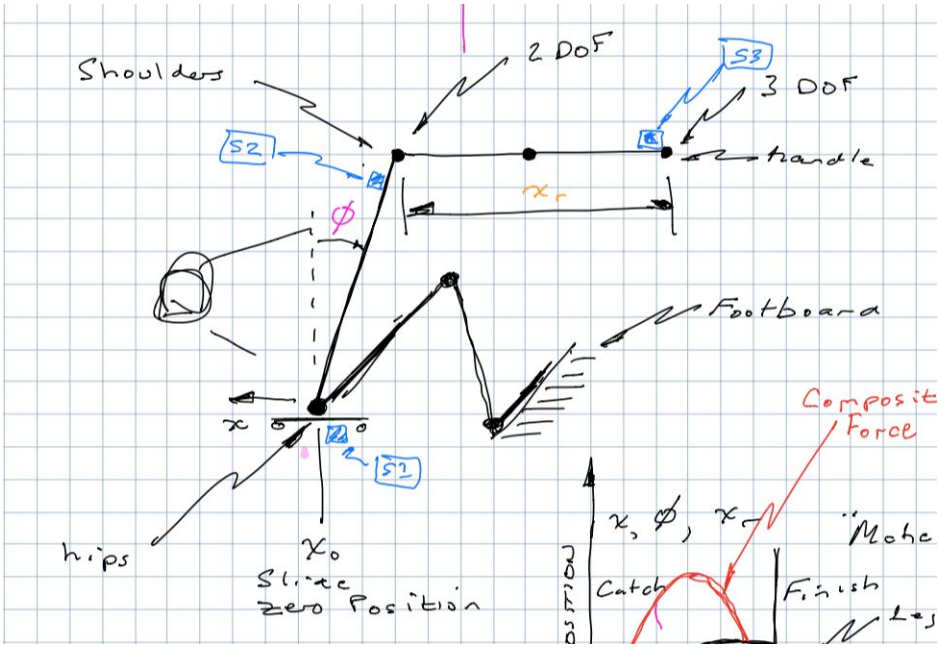

Figure 34. Diagram of rower and sensor placement on the rower.

By collecting data during rowing sessions, our team accumulated enough data. Having the data in csv files, our team could graph our data in different ways quickly. Then our team observed the data and interpreted its characteristics. In particular, how it compares to our proposed model. Shown in the figure 35 below are a few of the prototype graphs. These particular graphs are acceleration during the drive for each part of the stroke. These graphs allowed our team to assess whether or not the data needed to be interpolated in order to be clearer. These graphs are slightly underfit, but we were primarily interested in the trend of the data not the appearance.

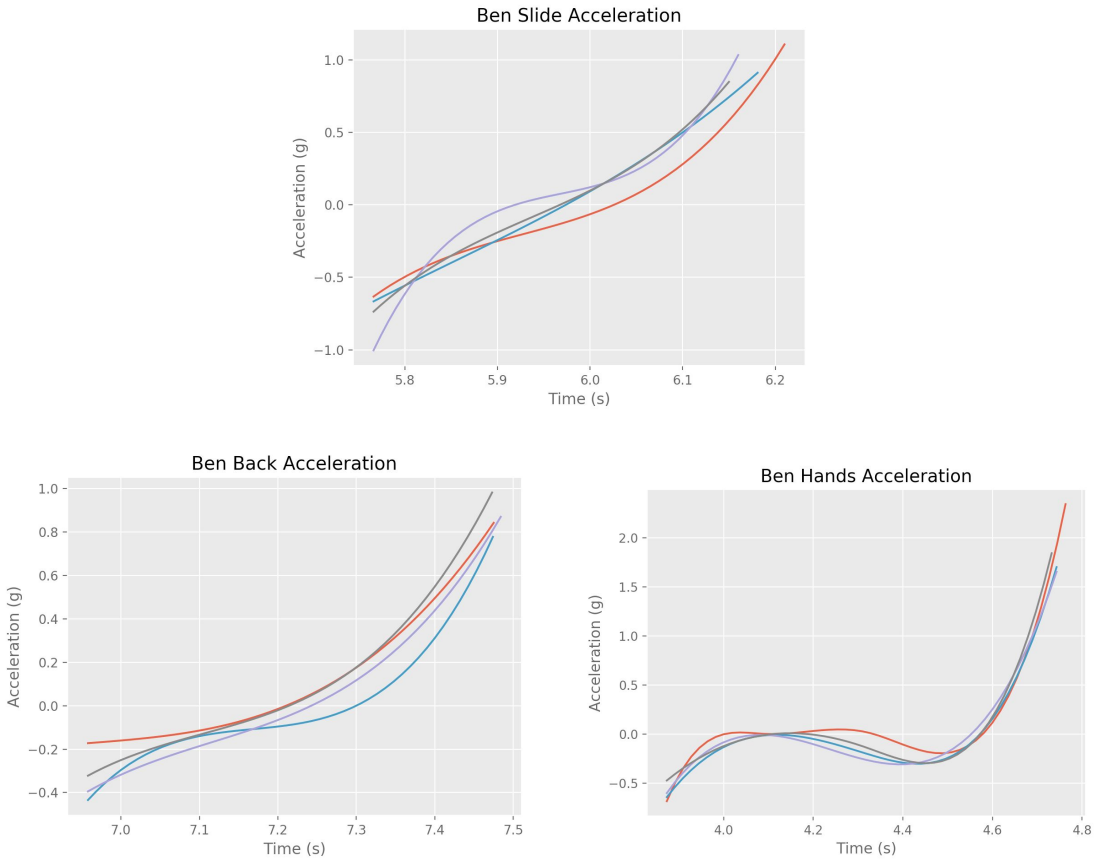

Figure 35. Graphs of individual strokes for each component.

Our next step was to overlay the three on the same graph. This enables our team to see the relative differences in acceleration for each sensor. There are two graphs that follow: figure 36 is raw acceleration data, and figure 37 is the acceleration values after applying our model calculations. The model is explained by the equations below.

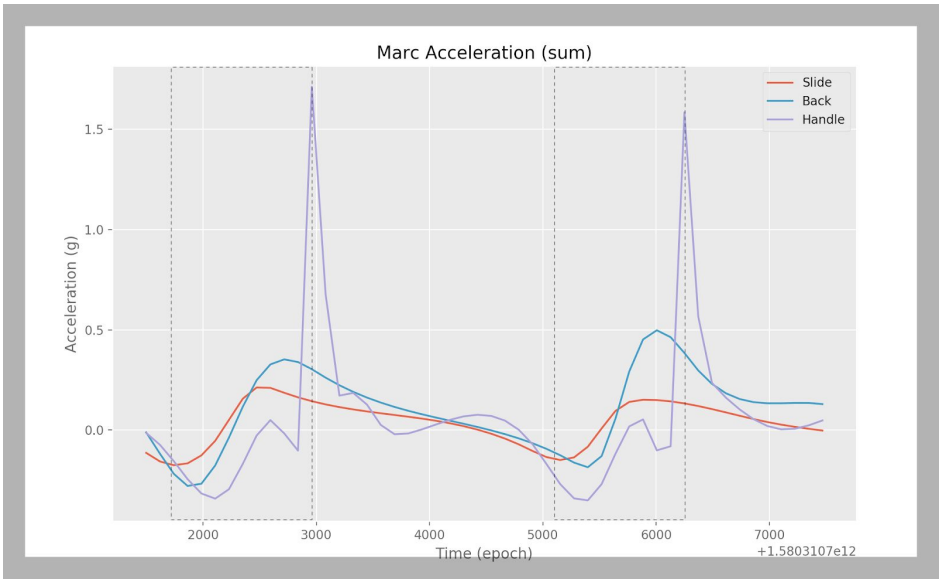

Figure 36. The raw acceleration data of each sensor during two medium pressure strokes.

Remembering the model, the *back* curve is a sum of both the accelerations of the *slide* and the *back*:

$$back_{sum} = back_{actual} + slide_{actual}$$

And the *handle* curve is a sum of all the accelerations of the *slide*, *back*, and *handle*:

$$handle_{sum} = handle_{actual} + back_{actual} + slide_{actual}$$

This is because they are all connected to each other by a body. Any acceleration that occurs on the slide also occurs on the back and handle because they are attached; and any acceleration that occurs on the back also occurs on the handle because they are attached. In example, the slide contributes to both the back and handle but neither back or handle contribute to the acceleration of the slide. In order to graph the acceleration generated by a particular part of the stroke, the back and handle must be adjusted.

The back must be adjusted by subtracting the slide:

$$back_{actual} = back_{sum} - slide_{actual}$$

The handle must be adjusted by subtracting the back and slide:

$$handle_{actual} = handle_{sum} - back_{actual} - slide_{actual}$$

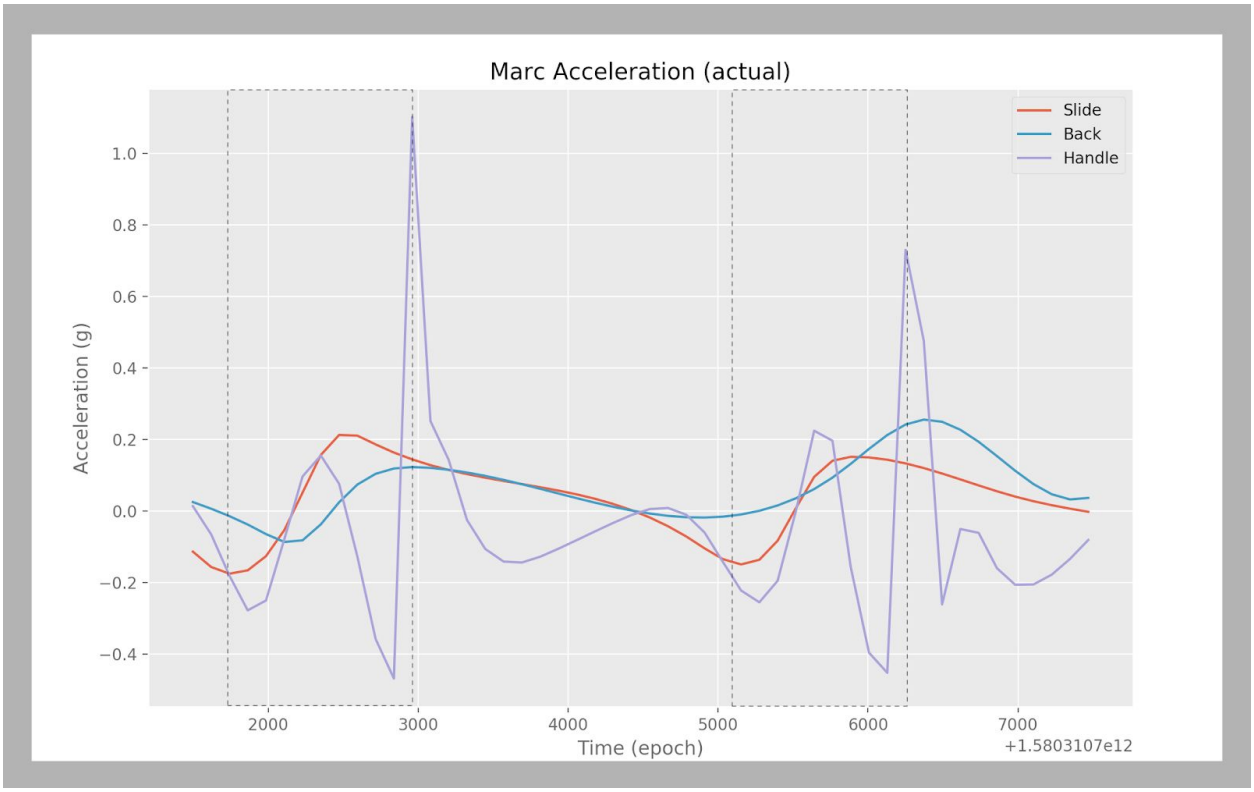

Figure 37. The actual acceleration data obtained by subtracting slide from back, and slide & back from handle.

This graph shows some information that was lost in the previous graph. The handle has a negative acceleration value on the drive, which is inside the dotted box. Notice how the slide stays the same as the previous graph, and the back and handle are adjusted to reflect their contribution. Although only two strokes are represented and there is only one rower participating, this is valuable information.

3.2.2 Coding Implementation

Our team chose the MetaMotionR sensor because it is small, wireless, and easily programmable in Python. The API is written in C with a python wrapper allowing the real time display code to be written in python. Python can be used to run a server, collect data via bluetooth in real time, and send that data to a client. It also has convenient libraries to visualize the data in the early stages.

Our team chose to collect the data on a small computer, Raspberry Pi, that runs on a Debian Linux based operating system called Raspbian. With a Linux distribution, our team could use the sensor API along with the Python bluetooth packages to write the program. The commands that came with the API enable the custom program our team wrote to both configure the sensor as well as stream data from the device. The Raspberry Pi can be seen in figure 38 below.

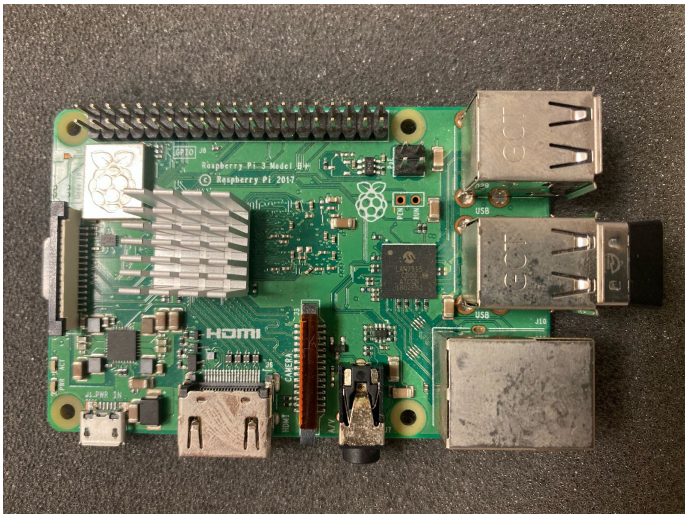

Figure 38. Raspberry Pi 3 Model B+, 2017.

In order to achieve real time data streaming, our team is taking the approach of using a web framework. In particular Django is being used as the framework of choice. The reason a web framework is very useful for real time streaming is because it allows the data visualization to be accessed from anywhere. Once the web server is started on the Raspberry Pi the stream can then be accessed from any web enabled device. Each time one of the sensors sends a piece of data to the Raspberry Pi the data is passed into Django. Then that data is sent to the client on a webpage using D3 to graph the data. D3 allows the binding of data to structures called document object models. Once bound, these document object models or DOAs can be manipulated in many different ways to create different graphs and visualizations of the data.

The main coding implementation challenge is that the processing time has to be fast enough so the user sees the graph before it's outdated. Since the rower is constantly taking strokes, data is relevant until the next stroke is taken. After that, the data is not live. There are three things that need to be accomplished while processing: 1. Transmit the data using bluetooth 2. Process and clean the data 3. Update the display. All these things need to happen during the recovery of the stroke so the data can be processed. Only then would the user be able to see the graph in time. This then allows the user to assess their technique in real-time. This was accomplished with a 2 second window for processing. The effectiveness of this will be addressed in a later section.

The secondary coding implementation challenge is drive detection. Since our team is only interested in the drive, there has to be a method to detect with acceleration data when the drive is happening (as opposed to the recovery). Some original ideas to do this involve using derivatives to find the maximum and minimum of the data which would give the beginning or end of the drive. Hence, finding the time at which the first derivative of acceleration (jerk) reaches 0 gives the start and of the drive. The jerk value at the beginning of the drive would be 0 because that is where the change in acceleration is 0. Each of these can be calculated from the

accelerometer data from the sensor. Unfortunately, this idea did not work well in practice however because of the dis-continuity of the data stream. To solve this problem, our team decided to display only one directional acceleration from the sensors. During the drive, acceleration values are positive and during the recovery they are negative. This is because the movements are in opposite directions. Choosing to display only positive acceleration values means only the drive is displayed.

The third coding implementation challenge is zeroing out gravitational acceleration. The gravitational pull of the earth influences the acceleration values because the sensors are accelerating 1g away from earth's center when lying still, shown in figure 39.

	A	B	C	D	E	F
1	epoc (ms)	timestamp	elapsed (s)	x-axis (g)	y-axis (g)	z-axis (g)
2	1.57919E+12	2020-01-16T11.22.20.013	0	0.023	-0.067	-0.997
3	1.57919E+12	2020-01-16T11.22.20.023	0.01	0.023	-0.067	-0.997
4	1.57919E+12	2020-01-16T11.22.20.032	0.019	0.023	-0.067	-0.997
5	1.57919E+12	2020-01-16T11.22.20.042	0.029	0.023	-0.067	-0.997
6	1.57919E+12	2020-01-16T11.22.20.053	0.04	0.023	-0.067	-0.997
7	1.57919E+12	2020-01-16T11.22.20.063	0.05	0.023	-0.067	-0.997
8	1.57919E+12	2020-01-16T11.22.20.073	0.06	0.023	-0.067	-0.997
9	1.57919E+12	2020-01-16T11.22.20.083	0.07	0.023	-0.067	-0.997
10	1.57919E+12	2020-01-16T11.22.20.094	0.081	0.023	-0.067	-0.997
11	1.57919E+12	2020-01-16T11.22.20.104	0.091	0.023	-0.067	-0.997
12	1.57919E+12	2020-01-16T11.22.20.114	0.101	0.023	-0.067	-0.997
13	1.57919E+12	2020-01-16T11.22.20.124	0.111	0.023	-0.067	-0.997
14	1.57919E+12	2020-01-16T11.22.20.135	0.122	0.023	-0.067	-0.997
15	1.57919E+12	2020-01-16T11.22.20.143	0.13	0.023	-0.067	-0.997
16	1.57919E+12	2020-01-16T11.22.20.154	0.141	0.023	-0.067	-0.997
17	1.57919E+12	2020-01-16T11.22.20.164	0.151	0.023	-0.067	-0.997
18	1.57919E+12	2020-01-16T11.22.20.174	0.161	0.023	-0.067	-0.997
19	1.57919E+12	2020-01-16T11.22.20.184	0.171	0.023	-0.067	-0.997
20	1.57919E+12	2020-01-16T11.22.20.195	0.182	0.023	-0.067	-0.997
21	1.57919E+12	2020-01-16T11.22.20.205	0.192	0.023	-0.067	-0.997
22	1.57919E+12	2020-01-16T11.22.20.215	0.202	0.023	-0.067	-0.997
23	1.57919E+12	2020-01-16T11.22.20.225	0.212	0.023	-0.067	-0.997
24	1.57919E+12	2020-01-16T11.22.20.236	0.223	0.023	-0.067	-0.997
25	1.57919E+12	2020-01-16T11.22.20.245	0.232	0.023	-0.067	-0.997
26	1.57919E+12	2020-01-16T11.22.20.255	0.242	0.023	-0.067	-0.997
27	1.57919E+12	2020-01-16T11.22.20.265	0.252	0.023	-0.067	-0.997
28	1.57919E+12	2020-01-16T11.22.20.275	0.262	0.023	-0.067	-0.997

Figure 39. Acceleration data without using sensor fusion. Sensor was placed still on a flat surface. Z-axis acceleration is approximately -1 despite no movement.

To solve this problem, our team has to utilize sensor fusion. The MetaMotionR sensor has a 3-axis accelerometer, 3-axis magnetometer, and a 3-axis gyroscope. We can determine the direction of the earth's center using the magnetometer, and determine the sensor's orientation with the gyroscope. Then we can subtract the gravitational acceleration vector (with magnitude 1) from the recorded acceleration vector to factor out gravity, shown in Figure 40.

	A	B	C	D	E	F
1	epoc (ms)	timestamp	elapsed (s)	x-axis (g)	y-axis (g)	z-axis (g)
2	1.57919E+12	2020-01-16T11.26.52.540	0	-0.001	-0.004	-0.035
3	1.57919E+12	2020-01-16T11.26.52.550	0.01	-0.001	-0.006	-0.039
4	1.57919E+12	2020-01-16T11.26.52.561	0.021	-0.001	-0.005	-0.039
5	1.57919E+12	2020-01-16T11.26.52.571	0.031	0	-0.005	-0.041
6	1.57919E+12	2020-01-16T11.26.52.581	0.041	-0.001	-0.006	-0.041
7	1.57919E+12	2020-01-16T11.26.52.590	0.05	-0.001	-0.006	-0.041
8	1.57919E+12	2020-01-16T11.26.52.600	0.06	-0.002	-0.005	-0.039
9	1.57919E+12	2020-01-16T11.26.52.610	0.07	-0.002	-0.005	-0.042
10	1.57919E+12	2020-01-16T11.26.52.621	0.081	-0.002	-0.007	-0.041
11	1.57919E+12	2020-01-16T11.26.52.631	0.091	-0.001	-0.006	-0.041
12	1.57919E+12	2020-01-16T11.26.52.641	0.101	-0.003	-0.006	-0.041
13	1.57919E+12	2020-01-16T11.26.52.651	0.111	-0.001	-0.008	-0.04
14	1.57919E+12	2020-01-16T11.26.52.662	0.122	0.001	-0.003	-0.041
15	1.57919E+12	2020-01-16T11.26.52.672	0.132	-0.003	-0.004	-0.041
16	1.57919E+12	2020-01-16T11.26.52.682	0.142	-0.002	-0.005	-0.04
17	1.57919E+12	2020-01-16T11.26.52.692	0.152	-0.001	-0.007	-0.042
18	1.57919E+12	2020-01-16T11.26.52.701	0.161	0.001	-0.006	-0.039
19	1.57919E+12	2020-01-16T11.26.52.711	0.171	-0.002	-0.005	-0.039
20	1.57919E+12	2020-01-16T11.26.52.722	0.182	-0.001	-0.005	-0.04
21	1.57919E+12	2020-01-16T11.26.52.732	0.192	-0.003	-0.003	-0.041
22	1.57919E+12	2020-01-16T11.26.52.742	0.202	-0.002	-0.003	-0.04
23	1.57919E+12	2020-01-16T11.26.52.752	0.212	-0.001	-0.005	-0.042
24	1.57919E+12	2020-01-16T11.26.52.763	0.223	-0.002	-0.006	-0.042
25	1.57919E+12	2020-01-16T11.26.52.773	0.233	-0.002	-0.007	-0.041
26	1.57919E+12	2020-01-16T11.26.52.783	0.243	0	-0.004	-0.041
27	1.57919E+12	2020-01-16T11.26.52.793	0.253	-0.002	-0.005	-0.04
28	1.57919E+12	2020-01-16T11.26.52.802	0.262	-0.003	-0.005	-0.039

Figure 40. Acceleration data using sensor fusion. Sensor was placed still on a flat surface. All acceleration values are close to 0.

Chapter 4: Design Process

4.1 Initial Client Statement

Based off of meetings with our sponsor Jon Rorke our team was presented with an initial client statement: “Currently, instrumentation of the rowing stroke timing elements is limited to a combination of rating, recorded in strokes/minute, power curves derived from machine or oar lock-based instruments, mirrors, videotape, and coaching feedback. What rowers need is a tool where they can receive individualized visualization of the three components of the rowing stroke: legs, back, and arms, in real time.”

4.2 Revised Client Statement

After meeting with the sponsor and further discussing what the goal of the application was; our team was given a revised client statement. The statement is as follows: “Develop an instrumented system to measure and feedback to the rower and the coach the timing and magnitude of the critical stroke elements individually for the legs, trunk, and arms throughout the catch and recovery phases of the stroke. The system should facilitate the real-time, intuitive observation by both athlete and coach and thus drive continuous stroke technique evolution. The measurements must be calibrated to a sufficient degree to allow valid long-term comparison over time and across rowers.”

4.3 Objectives

After reviewing the revised client statement our team created four objectives to meet as throughout the project. The first objective was to determine the viability of the proposed sensor placement through experimental sessions at The Practice Point Lab. Our team had an initial proposal of where the three sensors should be placed on the erg and rower in order to achieve the goal of breaking down the stroke however did not fully know if this sensor placement would work. This first objective was to use advanced three dimensional motion capture in order to prototype the sensor placement without having to go too much into the development process.

Our team's second objective was to collect real time data from three sensors on the rower and ergometer with a custom made program. This objective’s goal was to provide verification that a custom made program could collect data from three motion sensors. For this objective, our team was only looking to log data from the three sensors as an initial step and did not try to display that data in real time.

Our team’s third objective was to display real time data that breaks down timing of the legs, trunk, and arms. This objective is similar to our teams second objective however the difference is that this objective displays the data in real time not just logs it. This objective’s goal was to verify that real time graphing could be achieved using the hardware our team chose to

use. Our team was looking for a real time graph of each sensor's acceleration on a stroke by stroke basis.

Our team's fourth and final objective was to create a useful visualization to facilitate coaching on the ergometer. This final objective was set so that our team's custom made program would have a meaningful impact on the rower using the system. The goal of the visualization was to convey information that could give deep, substantial technique feedback to the rower and the coach that is also easy to interpret while under the stress of exercising.

4.4 Needs Analysis

From the data collected at PracticePoint and with the MetaMotionR sensors the user needs an interface where they can see live changes in the rowing stroke while rowing on the erg. The visualization should be intuitive and easy for the user to understand while exercising.

Our team conducted a pugh analysis to determine the viability of each design based on four design criteria. The design criteria used for this analysis were low cost, ease of use, ease of implementation, and effectiveness and accuracy. For our product the effectiveness and ease of use were the most important criteria with cost being the next most important and ease of implementation being the least. From this criteria our team decided that the real time data display was the best with an overall score of 48. The logged data design had a score of 33 and the design from PracticePoint had a score of 29. Table 3 shows the pugh analysis that our team created.

Table 3. Pugh Analysis

Criteria (Scored 0-4)	Importance Weights	Design 1 (Practice Point)	Design 2 (Logged Data)	Design 3 (Final Real time Data)
Cost	3	1	3	4
Ease of use	4	2	3	4
Ease of implementation	2	1	2	4
Effectiveness & Accuracy	4	4	2	3
	Scores:	29	33	48

Each of the scores are determined by multiplying each criteria by the importance. The importance factor was determined by the impact each had during the data collection periods.

4.5 Primary Conceptual Design

The first iteration of our project was created using data collected with Delsys sensors in PracticePoint. The sensors were placed on the seat and handle of the erg and the back of the rower. A graph of the acceleration of the rower overtime was created in Matlab. A separate graph was created for the acceleration of each sensor. However, the acceleration of the legs, body, and arms was not directly isolated because each sensor does not correspond directly to the acceleration of one body part. The primary design shows that it is possible to graph the acceleration of the primary parts of the rowing stroke using three sensors. The average acceleration for each sensor was graphed for one stroke (from catch to finish) with a standard deviation to show the consistency between strokes. Graphs were created for the four different stroke types (Adams, Grinko, Rosenberg, and DDR). In addition graphs were also created for two common bad techniques in rowing (shooting the slide and lunging at the catch). In figure 41 below you can see the graph of Adam style. Additional graphs of the other styles can be found in Appendix A.

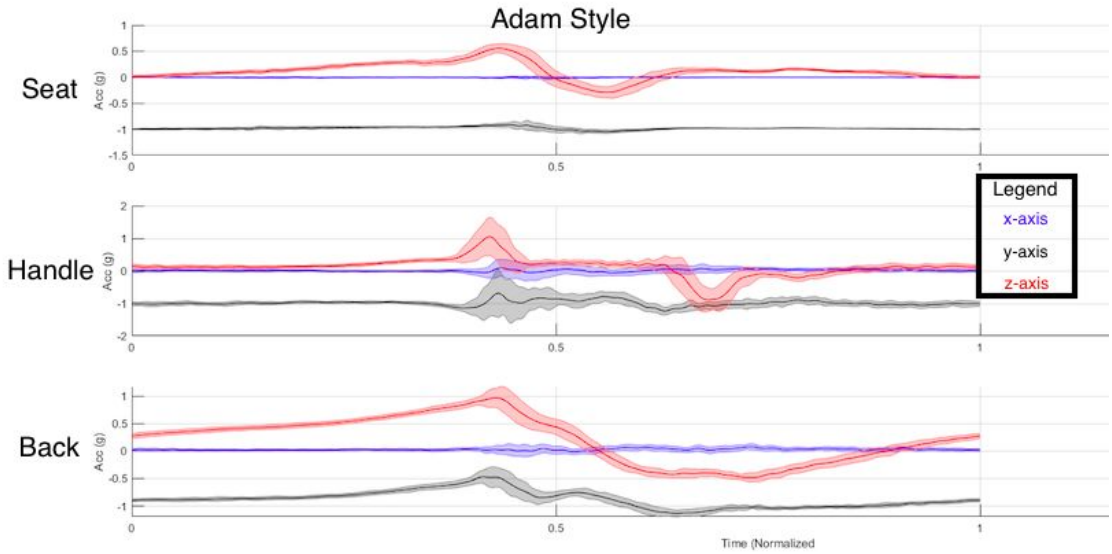

Figure 41. Acceleration vs. time for Adam Style.

In addition to creating a conceptual design for displaying acceleration data a conceptual design was also created for the position of the rower overtime. This data was collected using the Vicon motion capture system in PracticePoint. Graphs were then created of the change in leg position, back position, and arm position over the course of the stroke. These graphs were created by using the change in the angle of the knee, pelvis, and elbow respectively. The raw data was plotted first for each component so that the angle data could be visualized on separate graphs. The timing was then normalized so that all the components could be plotted on one graph. A graph of the average stroke was then compiled with the dark line being the average and

the shaded part showing the standard deviation between strokes. Figure 42 shows the raw data and figure 43 shows the combined graphs.

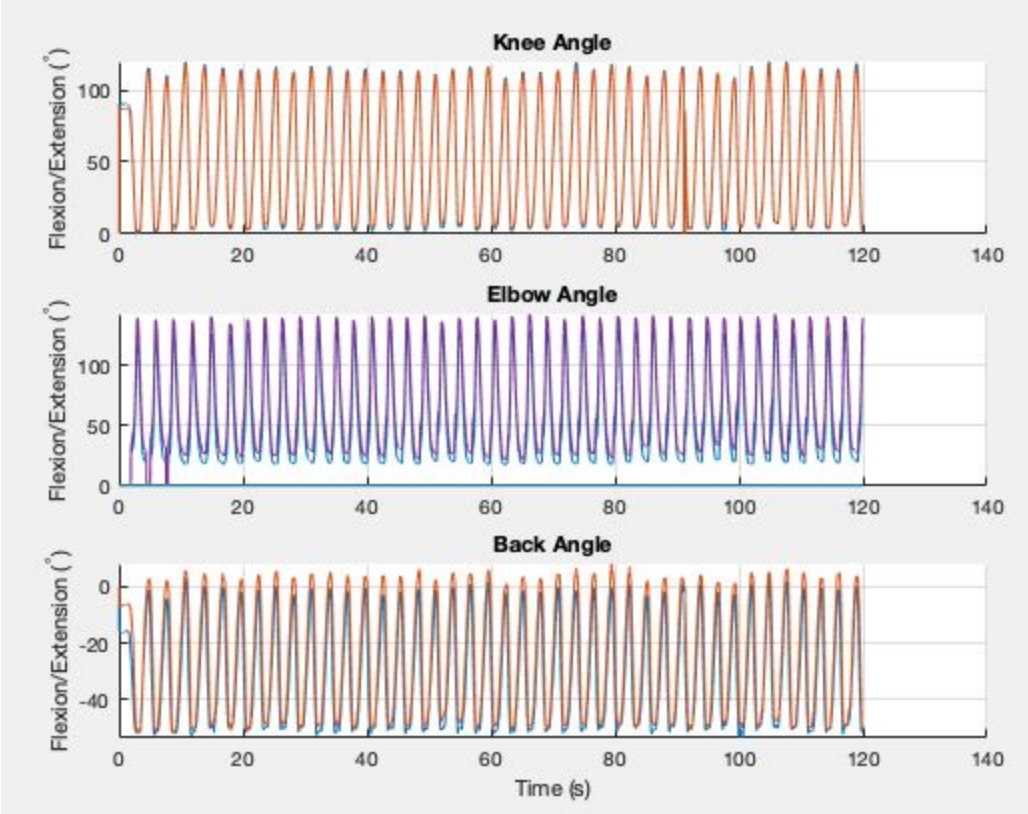

Figure 42. Raw position data from motion capture.

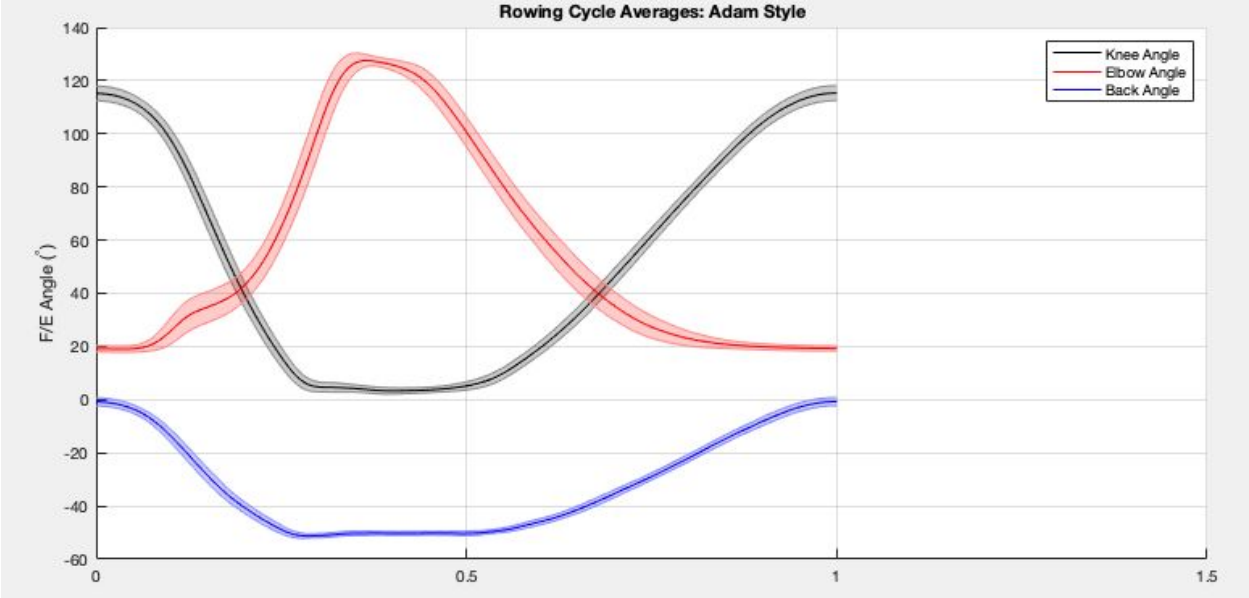

Figure 43. Position data with normalized time.

4.6 Alternative Conceptual Designs

The usefulness of visualized data lies in the interpretability of its visualization/model; how the user interprets the data depends on the interpretability of the visualization. Having a tool that can give a user a lot of data for the sake of data alone is not useful. The user must be able to derive meaning from what is being put in front of them. This concept is especially important with athletics. As specified, this tool is meant to be used in real time while the user is exercising. While under the intense physical exertion that rowing creates, the user may not be able to perceive a large, complicated volume of data. Therefore, it is important that we explore different forms to better visualize and to better translate the data.

Animation is frequently used for visualizing data over time to better understand the relationship between some variable and time. According to Robinson, Fernandez (Robinson and Fernandez, 2008) animation is more visually appealing and easier to understand than other types of data visualization. Our team hypothesized that animation could be applied to the visualization of the stroke. Using motion to represent physical motions might be useful for this project. This would give the rower a real-time animation of their own data; although it would likely increase the cognitive load. An example of this is shown in the graph in figure 44 below. The ball is a motion enabled object that moves with the subject. The speed of the object is controlled by the data gathered from the rower. An object for each element of the stroke would allow simultaneous comparison of their relative speeds. Each element is represented by an object. While prototyping this idea, our team determined it would not be possible. As mentioned previously, displaying data in real-time requires fast processing and given our computational limits it was determined that animation updates would be too much to compute in the <1-sec recovery period.

Figure 44. Animation for visualizing relative speed between objects--objects are in motion (Bostock, 2019).

A static form that we considered using is the stream graph. A stream graph uses area to convey the relationship between multiple categories. Below in figure 45 is an example of a stream graph. This particular stream graph shows box office shares of different movies over time. According to Robert Kosara (Kosara, 2016) the issue with stream graphs is that the irregularly shaped items stacked on top of eachother make precise readings difficult. In spite of this, the stream graph makes for an interesting look at the data. Our team explored this as a visualization technique for our project as it incorporated well the idea of general readings over precise readings. Each sensor would be a stream on the graph. This way a rower could look at the visualization and see generally how much of each piece their stroke was composed of. The stream graph has a flaw though; too many streams can cause the data to get cluttered and hard to read. Our team wants the display to be simple. When rowing at lower intensity, the rower could potentially absorb complicated figures and statistics but at higher intensities this is not possible.

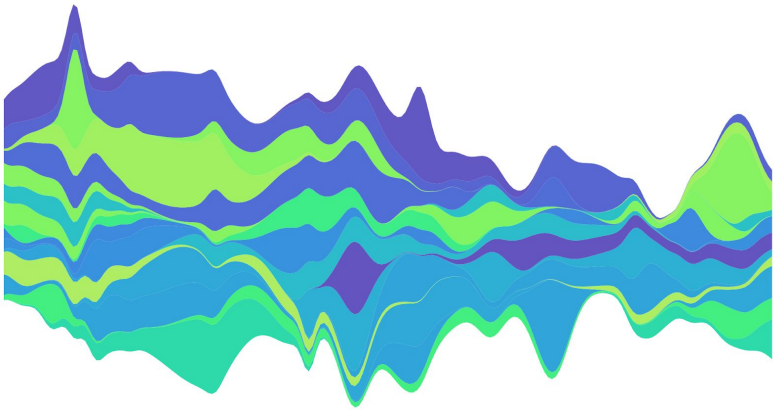

Figure 45. Steam Graph (Bostock, 2018).

Our team also considered variations of the bar chart. Two options were considered: the stacked bar chart (figure 46) and the grouped bar chart (figure 47). A stacked bar chart puts

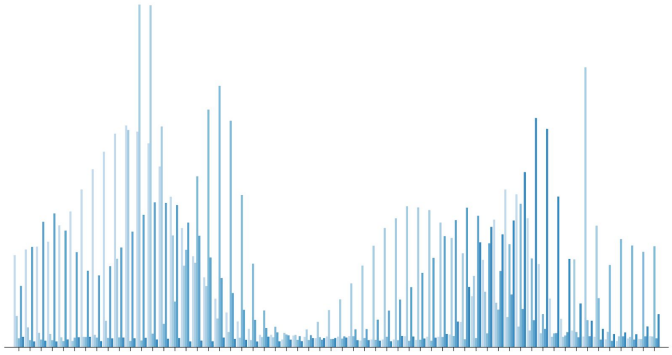

Figure 46. Grouped Bar chart (Bostock, 2018).

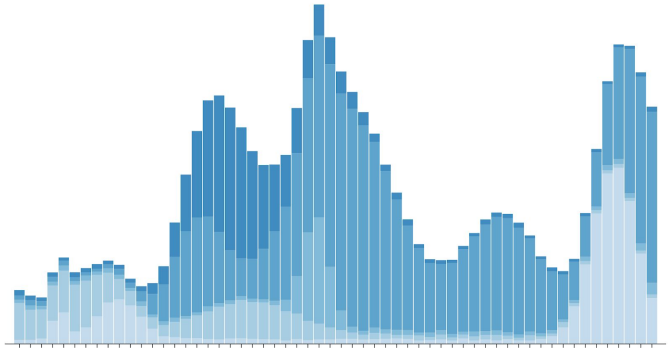

Figure 47. Stacked Bar chart (Bostock, 2018).

different categories on top of eachother while a grouped bar chart puts the different categories next to each other represented by different bars, shown below. Both types have benefits and drawbacks. With the stacked bar chart, the data from the three sensors would each be stacked on top of each other. With the grouped bar chart the data would be adjacent to each other. One of the easiest forms for visual comparison is length, which is a plus, but the grouped bar chart is better suited for quantitative measurements rather than relative (Ward, 2015). Our team was willing to sacrifice information load for simplicity. The stacked columns were simpler but ultimately we did not pursue it. The bar chart prototypes did not work for acceleration over time data because they were too busy, but they worked better for maximum acceleration. They allowed for quick, easily interpretable comparison of the three parts of the stroke. Also, from the bar chart experiments we learned that the stacking aspect of the stacked bars work well with the rowing stroke model, so we explored other stacking chart options and tried a stacked line chart. It seems to be a good compromise of simplicity and structure.

4.7 Final Design Selection

The stacked line chart is useful for interpreting the data, but we can update the style, format, and frequency of feedback to make it user friendly.

4.7.1 Form

Multiple coordinated views make understanding data easier (Convertino et al., 2003; North and Shneiderman, 2000; Roberts, 2007). For the sake of better understanding the stroke, having maximum acceleration on the display might be useful. Maximum acceleration is displayed above the stacked line chart as a bar chart. The bar chart (figure 48) drew out a positive correlation in the elements, maximizing complementarity between the two views (Baldonado et al. 2000). It is helpful to see an upward or downward trend over different timing elements.

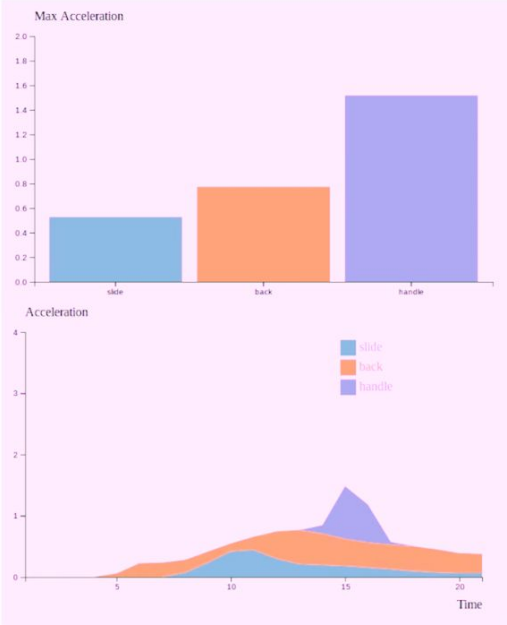

Figure 48. Real-time display.

As a bonus, the two views update in parallel so that the feedback is parallel, or coordinated. This can help them form a connection between the two views. This particular design is known as a dual view; the line chart provides an overview and the bar chart provides detail (Roberts, 2007), or an *Overview+Detail* view, opposed to *Focus+Context, Difference views*, and *Master/Slave.* An *Overview+Detail* view shows the whole dataset in one view and a piece of it in another view. *Focus+Context* shows a detailed bit of information with another view to give it context. *Difference views* are used to show the difference between two datasets. Difference views were used in figure 48 for design verification, as an example. Finally, *Master/Slave* is when some view controls the other view.

4.7.2 Style

The style in figure 48 is described as replacement (Roberts, 2007). Replacement happens when some new parameter changes the model and the new model replaces the old. Alternatives to this include overlay and replicate. Overlay happens when the new model is shown with the old model. Replication happens when the new model is displayed in a new window. Our team hypothesized that replacement would help the user focus on the current stroke while not diluting the information.

The style also uses color coded categories, keeping consistency across views. Encoding the categories with color helps the user identify the categories across views (Baldonado et al. 2000). The colors are also easily separable because of the ordering. The back is color coded as orange because 1. It makes it easier to see the difference between the elements. 2. It is a danger-zone for rowers in that too much use can cause injury. Choosing a color dissimilar to the others makes it so that changes are more likely to be seen.

Brushing is implemented as a tool for the coach to use. When brushing, the same elements are highlighted in both views simultaneously. Brushing is useful for identifying outliers (Lawrence et al. 2006), but with only 3 categories it was not difficult. The usefulness of brushing in this project was determined less than more, among a few tests.

Also, it is important to note the difference in complexity between the real-time visualization and the test visualizations. The real-time visualization received less data (~50 pts/update) than the test one (~400 pts/update), so interpolation was used for smoothing. However this caused drastic underfitting in the real-time visualization. A recommendation for any users of this system is to graph the saved data offline to get a better idea of the data, then the real-time visualization can be used more effectively. There are a number of examples within this document.

4.7.3 Frequency of Feedback

Looking into research on motor learning, which is a change in motor performance caused by training, concurrent feedback is effective in the early learning period (Liebermann et al., 2002), especially if the task is complex (Lee et al., 1990; Shea & Wulf, 1999; Snodgrass et al., 2010; Swinnen et al., 1997; Todorov et al., 1997; Wishart et al., 2002; Wulf et al., 1999; Wulf et al., 1998). However, when the learner is more experienced with the movement, they might benefit from less frequent, terminal feedback (Sigrist et al., 2012). Experienced users also might benefit more from terminal feedback because the task is no longer complex to them (Guadagnoli & Lee, 2004). Because the product is designed for high level athletes, terminal feedback seems to be the right choice. Below in figure 49 is an outline of the usefulness of several learning methods given task complexity.

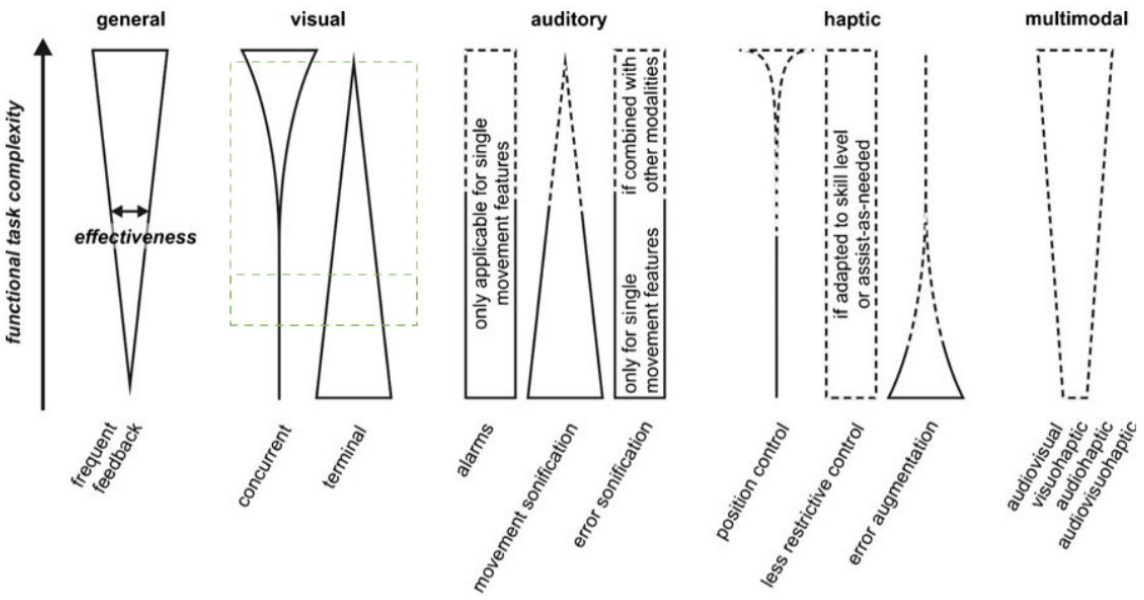

Figure 49. Effectiveness of feedback strategies with varying functional task complexity. Solid lines indicate experimentally confirmed and dashed is hypothesized (Sigrist et al., 2012).

The green highlighted area is where our team hypothesizes this project could live, depending on rower experience level. The smaller box indicates the specific target of this project, more experienced rowers. Concurrent feedback, had it been useful, would continuously update until the stroke ends. Figure 50 shows examples of what the display might look like. The three images are snapshots of the display; although they are not necessarily consecutive frames. Terminal feedback of the stacked line chart is shown in figure 51. The display only updates once the stroke ends. The top is an example of what it looks like during a stroke. The bottom is an example of what is on the screen after. The terminal feedback looks good, and based on the findings it is the better choice.

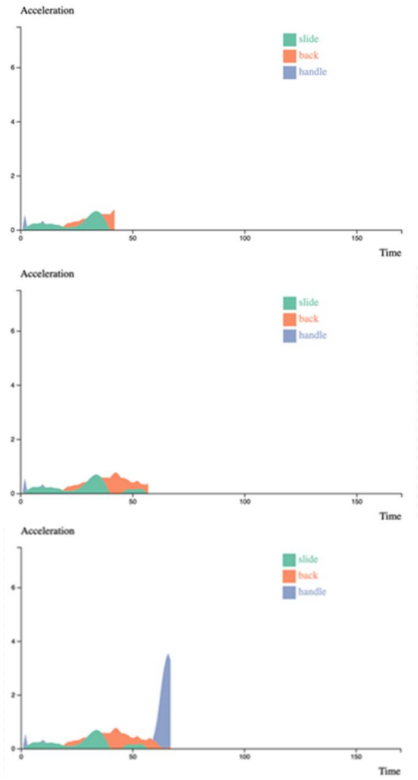

Figure 50. Concurrent feedback of the stacked line chart. The display updates continuously until the stroke ends.

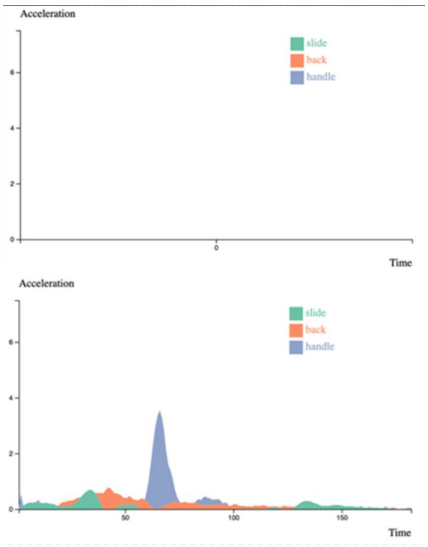

Figure 51. Terminal feedback of the stacked line chart. The display only updates once the stroke ends.

Chapter 5: Design Verification

5.1 Testing Procedures

To test the design, our team recorded data during multiple rowing sessions. To put together figure 52, our team manually picked out individual strokes from the sensor data csv file. Looking at the figure, it seems like there is enough variation between strokes to give coachable feedback--although not too much variation to bring up concerns. The sensors are fairly consistent with readings; so any major changes can be attributed to the rower.

Figure 53 is a stacked line chart. The green area shows the acceleration of the slide, the red area shows the acceleration of the back, and the blue area shows the acceleration of the handle. Before looking at the chart, our team expected to see acceleration in this order: slide, then back, then handle as this corresponds to the sequence of the rowing stroke.

Looking at the chart, our team's hypothesis is tentatively confirmed. At first the slide is the only acceleration seen, indicating that the legs are the only part of the body accelerating and contributing to the stroke. In the next part of the stroke the back adds to the acceleration of the stroke while the slide acceleration decreases. Finally, after the back decelerates the handle accelerates dramatically. That is consistent with the hypothesis and also consistent with the graphs in section 3.2. However, sometimes at the beginning there are seemingly random bumps. For example, in the bottom right of figure 53 there are red and blue bumps at the beginning.

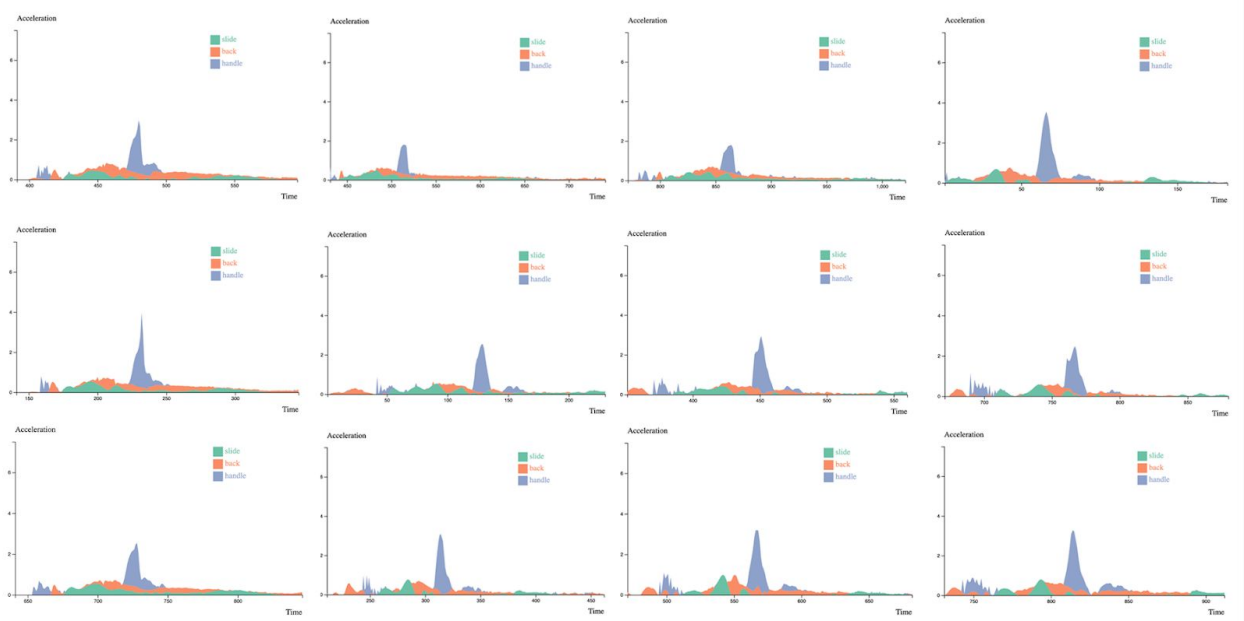

Figure 52. 12 strokes randomly taken from 4 different rowing sessions. Green is the slide, Red is the back, and Blue is the handle.

These are actually explainable by bad rowing techniques. If there is a red bump too early, this is called opening the back. When a rower opens their back, the back is initiated before the legs. In addition, if there is a small blue bump too early the rower grabbed at the catch. Grabbing at the catch is when a rower begins the stroke by pulling with their arms.

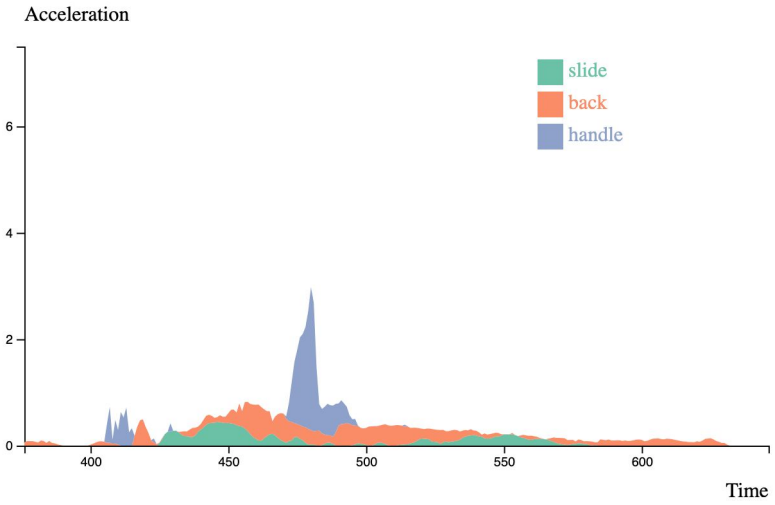

Figure 53. Closeup of one of the strokes.

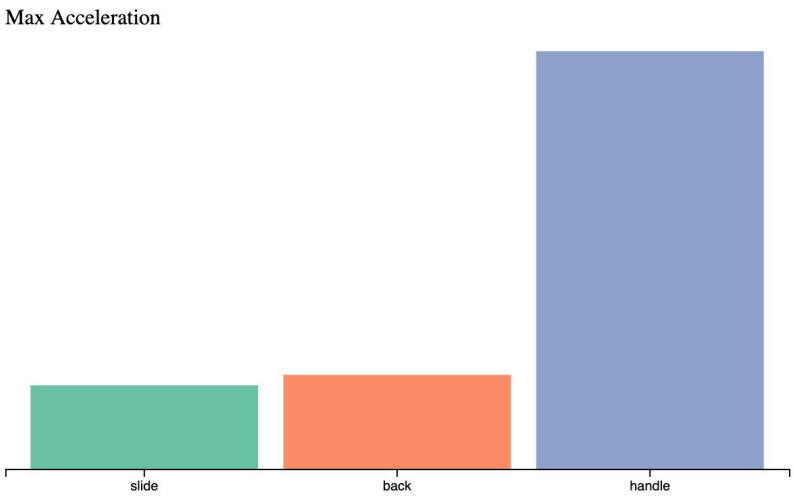

Figure 54. Maximum acceleration over 1 stroke.

Looking at maximum acceleration of this stroke in figure 54, the slide and back are relatively equal while the handle definitely reached a higher acceleration. Although the handle has a higher peak acceleration, it is only maintained for a brief period whereas the slide and back have longer maintained acceleration. After looking at this stroke, a coach might notice that the

rower opened the back slightly at the catch (the red bump before the slide starts). So they might tell the rower to use the legs more at the catch. Other than that, everything else seems to be in order. Looking at another stroke in figure 55, a coach might notice that the rower was shooting the slide. Shooting the slide is when a rower pushes the legs without swinging the back and arms. This is indicated by the sharp decline of the slide acceleration followed by a sharp increase in back acceleration. In this case, even though it is not optimal it is not that bad because the back curve starts before the slide curve ends. If the back started after the slide ended, then that would be worse as the rower would have discontinuity in their movements. Although we do not know for certain if during this particular stroke the rower shot the slide, the data strongly suggests that they did. This is an example of how general knowledge of the rowing stroke can be applied to interpret the results from the visualization.

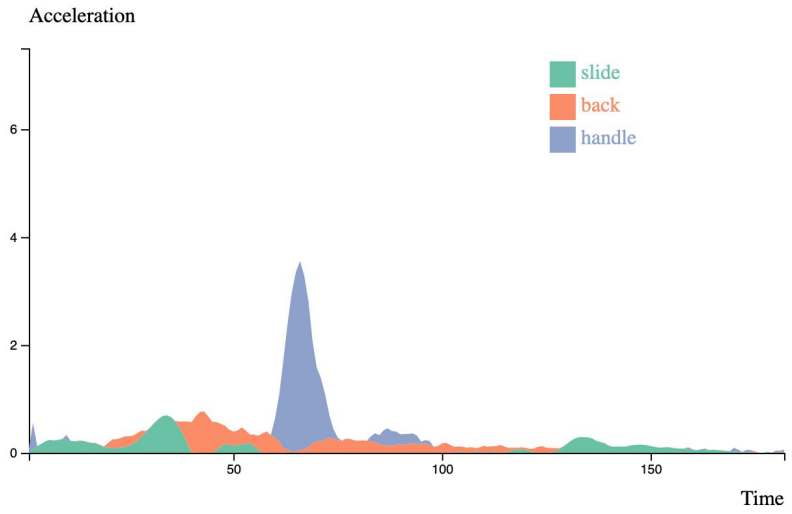

Figure 55. Closeup of one of the strokes.

Chapter 6: Final Design and Validation/Results

6.1 Experimental Methods

Experimental data was extremely important both for providing preliminary visualization as well as providing an accurate biomechanical model of the rower. Experimental data was captured initially by utilizing Practice Point, a state of the art motion capture facility on the WPI campus.

The Practice Point facility at WPI was equipped with a room at Infrared Cameras that were used to track the motion of reflective markers on a subject's body. Motion was tracked and measured using the Vicon Plug-in-Gait software. This software allowed us to extract position and motion data from each session and visualize it by applying a butterworth filter to the motion and graphing it. There were 40 reflective markers on the subjects body, these were meant to measure the exact position of the subject through the entire stroke cycle. Utilizing the Practice Point Facility and the Vicon software gave us much more data than what our MEMS sensors gave out, the results from both are comparable.

The experimental data from the early test sessions with our MEMS sensors provided helpful insight as to what needed to change moving forward. The original sensors were put through prototype testing that involved taping the bulky sensors to the subject and observing the data. After several initial tests, the group decided to adopt a more compact accelerometer.

6.2 Data Analysis Final Product

Collecting real-time data with the final design proved to be difficult with the data-loss and timing issues. Nevertheless, the data was comparable to every other offline session. Figure 56 shows two consecutive strokes on the display. For this rower, elements of the stroke seem to be building upon each other. When the previous element reaches a maximum, the next element adds on significantly. The maximums are marked in the figure on the left. On the right, the last element does not build off the previous indicating that there was deceleration and most likely loss of power. Being able to recognize this pattern is possibly the most useful feature of this visualization. If the building stops before the stroke ends, there must be a coachable movement that corrects this.

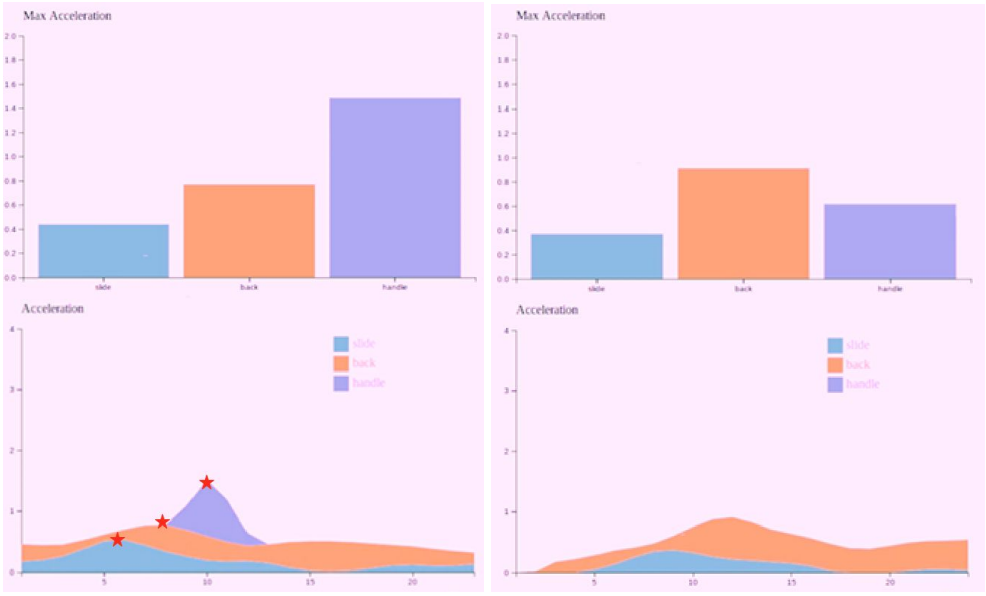

Figure 56. Real-time display updated over two consecutive strokes.

6.3 Data Analysis Biomechanics

In order to show that there was a significant difference between the well executed and poorly executed rowing strokes the team conducted a t-test in Excel. The team used the following data to conduct the t-test. The data in table 3 was inputted into the t-test function in Excel.

Table 4. Data used to conduct t-test.

Input Values			
Data set 1	Data set 2	Number of tails	Type
Adam acceleration	Rushing acceleration	1	2

A t-test was conducted between the slide acceleration of the Adam Style, with the Rosenberg and Grinko style and Rushing the slide data. The t-test showed that there was no significant difference between the slide acceleration of the Adam and Rosenberg style and the Adam and Grinko style. However, there was a significant difference between the slide acceleration of the Adam style and the Rushing the slide data. These results were what the team expected. The team did not expect a significant difference between the three rowing styles. This is because the difference between these styles is how the legs and back are emphasized during the stroke which only minimally affects the acceleration of the slide. Rushing the slide is a common poor technique that some rowers develop as they are learning how to row. It is when the slide accelerates backwards before the handle and back of the rower moves. When rowers rush the slide the acceleration increases drastically. Therefore, it was expected that there would be a significant difference between the slide acceleration of the Adam style and the slide acceleration of the rushing the slide data.This can be seen by the p-value of 8.44e-06. The p-values between

the other stroke types can also be seen in table 4 below. A close up of the comparison of the slide acceleration of the Adam style and rushing the slide can be seen in figures 57 and 58 below.

Table 5. P-values generated in Excel.

p-values (seat)		
Rushing	Rosenberg	Grinko
8.44E-06	0.213	0.320

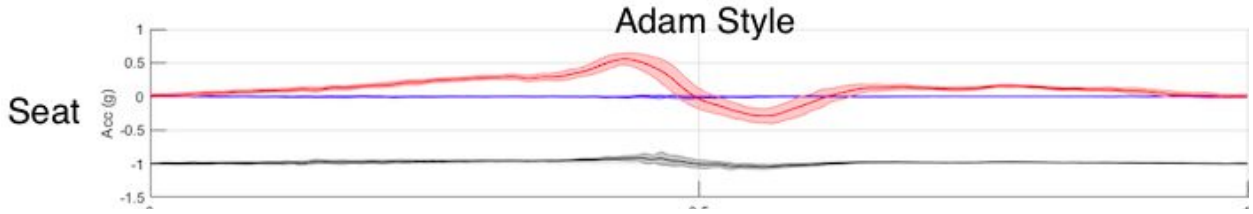

Figure 57. Slide acceleration of Adam style.

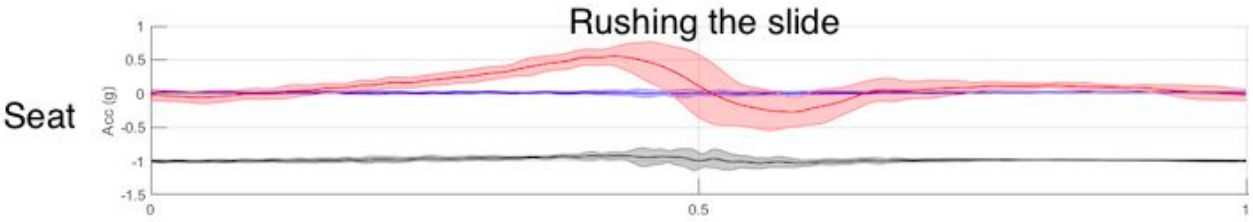

Figure 58. Slide acceleration of rushing the slide.

6.4 Product Impacts

This section contains theoretical product impacts as the team does not have an actual product.

6.4.1 Economics

The price of this product is competitive with the current devices on the market. The top competitor of our product is BioRow which costs 500 euros, approximately 541 USD (as of April 27, 2020 1 euro=1.08 USD). Our product consists of 3 sensors which each cost approximately 100 USD. However, if this device were mass produced then that would substantially reduce the cost of our product. The manufacturing costs of our product would also be minimal. Another competitor is the technology that is currently on the erg itself. Since both our product and BioRow are used as an add on for the erg there is a big jump in cost. However, the technology in our product exceeds what the erg itself can do and therefore the benefits are able to outweigh the cost difference.

6.4.2 Environmental Impacts

Our product has minimal impacts on the environment. The sensors that are being used are already being manufactured for other products as well. Therefore any environmental impacts that occur from the production of these sensors are not directly related to our product. The sensors are also recyclable; the outer casing of the sensor is made of plastic and therefore can be recycled in the normal recycling stream. The internal electrical components can be recycled at an electronics recycling center and the lithium ion batteries can also be recycled. The battery is also rechargeable so it will last 2-7 years before it has to be replaced. A device to attach the sensors to the rower and erg also needs to be created but this can be designed and 3D printed. Therefore there would also only be minimal to no environmental impacts from this process.

6.4.3 Social Influence

This product will have an impact on the rowing community. This product is specifically targeted towards rowers and coaches and therefore most likely will not impact the general population. Ideally the device will help improve rowers technique and therefore could have an impact on the rower's rowing performance. The tool is created to assist rowers when training on the erg but the benefits of the product will be able to be seen in the timing of the rower's stroke on the water as well. In the future a tool like this could also be developed for running and other aerobic activities. It could help all athletes to stay on top of their training. This is especially something to consider during the pandemic that we are currently living through. Athletes will not have access to their coaches and the general population is trying to stay active, so an app that will help them improve their technique and reduce injuries would be beneficial. It could make activities like rowing, running, and biking more mainstream. This is important, more so than ever, during this global pandemic where society is moving inside.

6.4.4 Political Ramifications

There are no political ramifications of this product as the team does not currently plan on making the product available internationally. If in the future the product becomes available internationally then there could be potential political ramifications as our top competitor's product is based in the United Kingdom. However, although our product has a similar goal to this product the technology used to create it as well as the visualization outcome is completely different. Therefore it is extremely unlikely that there will be any political ramifications.

6.4.5 Ethical Concerns

There were no ethical concerns associated with this product. The product was tested on humans (only within the project team); however, the only devices that the human came in contact with were the wearable sensors. These sensors are already manufactured to be worn by humans

and therefore there were no harms associated with this product. Due to Covid-19 the team was unable to complete further testing of the product. However, if further testing was conducted with outside test subjects then our team would have gone through the IRB process and created an informed consent form for all participants, that would have remained confidential. Any data that would have been used from these studies would have remained anonymous

6.4.6 Health and Safety Issues

The health and safety issues associated with this project do not exceed the health and safety issues associated with the sport of rowing. As with any sport or exercise there is always the risk of injury if not conducted properly. However, the addition of three sensors does not increase the health and safety issues associated with rowing. There is even the possibility of reducing these risks as the technology will help improve the rowers technique and reduce the likelihood of injury occurring from improper technique. Being able to notice the differences between the graphs can also lead to good injury prevention techniques. An athlete would be able to identify a common mistake and potentially avoid an unnecessary injury. The sensors generate, use, and radiate radio frequency energy and therefore if they are not installed correctly then they could have interference with radio connections.

6.4.7 Manufacturability

The manufacturing associated with this product is minimal. The product uses sensors that have already been manufactured. The sensors are coded to work together to get the desired outcome which will be displayed through an app. Therefore, the physical manufacturing process is minimal. One thing that will have to be manufactured is the housing for the sensors that will allow for a better connection between the user and the program. This can be manufactured easily using manufacturing techniques such as 3D printing. The fixture could be manufactured using ABS plastic which costs $25 per a kilogram. The sensor is approximately 1.5in x 1in x 0.5in; therefore we could say that the housing would use approximately 1in^3 of filament. The density of ABS is 1.07 grams/cm^3, so 1kg of filament would give a cubic area of 934 cm^3 (57 in^3). Therefore each housing unit would cost less than $0.50 to manufacture. The team created a bill of materials (BOM) and cost of goods sold for the product (COGS), which can be seen in tables 5 and 6 below.

Table 6. BOM for the final product.

Part Number	Part Name	Material	Cost	Amount	Quantity of Part	Total Cost
1	MEMS sensors	electronic components	$63.99 per sensor	n/a	3	$191.97
2	Sensor housing	ABS plastic	$25/1kg	1 in^3	3	$1.32
3	Strap	polyester and rubber	$13.50/10 yards	1 yard	1	$1.35
4	Clip	ABS plastic	$25/1kg	0.25 in^3	2	$0.22

Table 7. COGS for the final product.

Weekly Rate	Material Base Cost	Material Acquisition Cost	Material Cost	Labor (min)	Labor Cost ($/hr)	Yield %	Total Cost/Unit	Unit Lot Charge	GM %	GM $	Price/Unit
1000	$194.86	0.15	$224.08	60	75	0.95	$314.82	$10	0.4	$125.93	$450.75

6.4.8 Sustainability

This product has no additional sustainability concerns. As mentioned in the environmental concerns section the impacts would not be directly related to our product since the sensors are already being manufactured for other uses as well. The only additional manufacturing process that is being used is 3D printing which is a sustainable process since it can be completed using recycled materials. 3D printing also reduces waste since it only uses the necessary material.

Chapter 7: Discussion

7.1 Product Feasibility

With only several tests done, the product seems feasible. Unfortunately testing of the final iteration was limited to within the team because of the global pandemic effective during D-term of 2020. However, in the tests completed the visualization seems to vary more by rower than intra-rower strokes. This does not help narrow the search for optimal timing of the stroke elements, but it tells us that doing an inter-crew comparison might result in valuable feedback. Novice rowers have more variation in their strokes than well trained rowers (Bosch, 2015), but an analysis between two or more well trained crews might provide insight into timing differences that affect performance. There are a few more steps to take before a comprehensive analysis can be conducted, such as programming the separation of strokes, but this project created a means to dissect the timing elements.

As a product, it is still in the development phase. It is entirely possible that it could be a usable product in a few years, but it is important that an analysis is conducted on high level rowers timing elements to determine product impact. Although the current measurement system is probably not precise enough to see acute differences between the strokes of a well trained rower, it is precise enough to see differences between rowers. If differences in timing between well trained rowers are related to performance success, then that would make this an invaluable product to high level crews.

7.2 Design Limitations

During testing of the real-time system a few limitations were noticed. The first being the manner in which the sensors were mounted. The three sensors are mounted to the rower and erg with athletic tape for ease of attachment in different positions. But mounting with tape blocks bluetooth data transfer down to ~15% of the original dataset. Sparsity causes inaccuracies in the display and a definite underfit of the small dataset. This could be prevented in future iterations by devising a better mounting method that minimally covers the sensors. Some ideas are 1. A chest strap that enables detachable sensors. 2. A clamp that attaches to the erg handle and enables detachable sensors. 3. A clamp for the seat that enables detachable sensors.

The second design limitation originates from the timing constraint for processing. In order to update the display for every stroke, our team decided to collect data, process, and update the display in set time intervals; we decided 2 seconds was appropriate. Every 2 seconds the program resets the graph to display the next stroke. 2 seconds is near the average time for a rower to take a stroke at ~25 strokes per minute. As a consequence, if the rower is not rowing around 25 strokes per minute then they will only see part of the stroke on the display. With higher stroke rates a single stroke takes a shorter amount of time so the stroke might show up in full on the display. With lower stroke rates a single stroke takes as long as 4 seconds to complete

which would only show about half the stroke on the display. Solutions for resetting the graph upon stroke completion could be 1. Using local maxima to identify the start and stop of the stroke, thus extracting the full stroke from the data. 2. Transfering data in small chunks (~10 points) and as they arrive check for Gaussian anomalies. 3. Use machine learning to identify telling features. These features are like where the catch is located or where the finish is located.

Chapter 8: Conclusion and Recommendations

8.1 Conclusions

Overall our team accomplished all objectives defined. The first objective was to determine the viability of sensor placement through experimental sessions at The Practice Point Lab. Through data collection sessions at Practice Point our team was able to determine that the three sensors were sufficient to classify the rowing stroke. Furthermore, three sensors placed on the handle and slide of the erg as well as on the back of the rower was enough to derive detailed information about the stroke from the data. This information can show technique deficiencies as well as show the amount of acceleration each part of the body is contributing to the total acceleration of the stroke.

Our team's second objective was to collect real time data from three sensors placed on the rower's body and the ergometer. This goal was accomplished by our team during the preliminary design phase. As seen in section 3.2.1 during the prototyping phase of development our team was able to log acceleration data from the three sensors into a csv file then graph them using matlab. Completing this objective allowed our team to visualize what the data of the stroke looked like together and be able to start to brainstorm how that data could be visualized.

Our team's third objective was to display real time data that breaks a rowers stroke down into slide, trunk and handle acceleration. This objective was completed in the final iteration of our team's developed application. As seen in section 5.1 figure 52 the final application was able to display the three elements of the stroke in real time. These visualizations are displayed on a stroke by stroke basis as the rower is rowing.

Finally, our team's fourth objective was to create a useful visualization of the acceleration data to facilitate coaching on the ergometer. Completion of this objective can be seen again in section 5.1 figure 52 where a stacked line chart and bar chart was used in the final visualization of the acceleration data. These visualizations utilized color and height to differentiate between the three different accelerations of the legs, trunk, and back. The visualizations are both easy to understand for a rower who is exercising while also giving depth of information to give valuable technique feedback to both the rower and the coach.

8.2 Recommendations/Topics of Future Research

Future projects can continue what this project has initiated by using machine learning. Machine learning could have a few applications for analyzing the rowing stroke. One idea is to classify good versus bad strokes. The coach could train a model with a prefered style in mind and while the rower is rowing he would give feedback whether or not that stroke was in the coaches prefered style. A major consideration for any team that pursues this idea is that style varies

largely by person. So in order to properly classify a stroke within a large category, say Adams style, then it is likely that they will need 100 or more rowers to cast a net that is wide enough.

Another idea is to classify a stroke as injury prone or not injury prone. The coach could train a model to identify injury prone strokes which would signal to the coach that the rower is using an injury prone style. This would have the added benefit of training a rower with theoretically safer/better rowing techniques. To implement this, a large amount of data would be needed to train the algorithm.

Another topic of future research could be exploring alternative visualization techniques to the ones used in this project. There are still many aspects that could be improved. Concepts such as optimal color usage, more effective forms, and the limit to the amount of information a rower can absorb while exercising. It might be especially interesting to explore 3D visualizations for rowing data. It is definitely possible to visualize the stroke in 3D, but we are not sure what forms might be useful for feedback. It is possible that 3D surfaces could represent the stroke better. All of these ideas would benefit from more testing with high-level rowers. There are many paths to follow. We believe that any of these paths would be both interesting and original.

References

A BEGINNER'S GUIDE TO ROWING AND THE BENEFITS. (n.d.). Retrieved October 8, 2019, from https://www.jebiga.com/benefits-rowing/.

Baca, A., & Perl, J. (2019). Modelling and simulation in sport and exercise. Retrieved from https://books.google.com/books?hl=en&lr=&id=NHxqDwAAQBAJ&oi=fnd&pg=PT74&dq=biomechanics of rowing&ots=93WBPyn37A&sig=xDnrUv1Nr7rGnH4GeNZtC3ssi7A#v=onepage&q=biomechanics of rowing&f=false

Baldonado, M. Q., Woodruff, A., & Kuchinsky, A. (2000). Guidelines for using multiple views in information visualization. Proceedings of the Working Conference on Advanced Visual Interfaces - AVI '00. doi:10.1145/345513.345271

BioRow Systems. (n.d.). Retrieved May 13, 2020, from http://biorow.com/products/biorow instrumentation/

Bosch, S., Shoaib, M., Geerlings, S., Buit, L., Meratnia, N., & Havinga, P. (2015). Analysis of Indoor Rowing Motion using Wearable Inertial Sensors. Proceedings of the 10th EAI International Conference on Body Area Networks. doi:10.4108/eai.28-9-2015.2261465

Bostock, M. (2018, October 23). Stacked-to-Grouped Bars. Retrieved May 10, 2020, from https://observablehq.com/@d3/stacked-to-grouped-bars?collection=%40d3%2Fd3-transition

Bostock, M. (2018, September 06). Streamgraph Transitions. Retrieved May 10, 2020, from https://observablehq.com/@d3/streamgraph-transitions

Bostock, M. (2019, August 17). Easing Animations. Retrieved May 10, 2020, from https://observablehq.com/@d3/easing-animations?collection=%40d3%2Fd3-transition

Breiland, M. (2017, March 1). Improving Your Rows with the Force Curve. Retrieved April 30, 2020, from https://www.concept2.com/news/improving-your-rows-force-curve

Breiland, M. (2018, May 22). What Is The Ideal Rowing Stroke? Retrieved October 8, 2019, from https://www.concept2.com/news/what-ideal-rowing-stroke.

Černe, T., Kamnik, R., & Munih, M. (2011). The measurement setup for real-time biomechanical analysis of rowing on an ergometer. Measurement, 44(10), 1819–1827. doi: 10.1016/j.measurement.2011.09.006

Cheri. (2019, August 2). Technique Videos. Retrieved October 8, 2019, from https://www.concept2.com/indoor-rowers/training/technique-videos.

Convertino, G., Chen, J., Yost, B., Ryu, Y., & North, C. (2003). Exploring context switching and cognition in dual-view coordinated visualizations. Proceedings International Conference on

Coordinated and Multiple Views in Exploratory Visualization - CMV 2003 -. doi:10.1109/cmv.2003.1215003

Empacher Racing Eight. (n.d.). Retrieved March 4, 2020, from https://www.empacher.com/en/products/racing-boats/empacher-racing-eight/

Geer, J. (2018, June 6). What is an Erg? Retrieved from https://www.concept2.com/news/what-erg.

Guadagnoli, M. A., & Lee, T. D. (2004). Challenge Point: A Framework for Conceptualizing the Effects of Various Practice Conditions in Motor Learning. Journal of Motor Behavior, 36(2), 212-224. doi:10.3200/jmbr.36.2.212-224

Herniated Disc Treatment – Santa Monica's Disc Pain Expert. (n.d.). Retrieved May 15, 2020, from https://drjustindean.com/services/herniated-disc/

Hosea, T. (n.d.). Orthopaedics & Physical Performance. Retrieved January 29, 2020, from https://www.urmc.rochester.edu/orthopaedics/sports-medicine/rowing-injuries.cfm

Hosea, T. M., & Hannafin, J. A. (2012). Rowing Injuries. Sports Health: A Multidisciplinary Approach, 4(3), 236–245. doi: 10.1177/1941738112442484

Kleshnev, V. (2005). Comparison of on-water rowing and its simulation on Concept2 and Rowperfect machines. Scientific proceedings: XXII International Symposium on Biomechanics in Sports, Beijing. pp 130-133.

Kleshnev, V. (2016). The Biomechanics of Rowing. Ramsbury, Marlborough, United Kingdom: Crowood Press Ltd.

Kosara, R. (2016). Presentation-Oriented Visualization Techniques. IEEE Computer Graphics and Applications, 36(1), 80–85. doi: 10.1109/mcg.2016.2

Lawrence, M., Lee, E., Cook, D., Hofmann, H., & Wurtele, E. (n.d.). Exploratory Data Analysis of Systems Biology Data. Fourth International Conference on Coordinated & Multiple Views in Exploratory Visualization (CMV'06). doi:10.1109/cmv.2006.7

Lee, M., Moseley, A., & Refshauge, K. (1990). Effect of Feedback on Learning a Vertebral Joint Mobilization Skill. Physical Therapy, 70(2), 97-102. doi:10.1093/ptj/70.2.97

Lei, A. (2011). Application of accelerometers in the sport of rowing. (Doctor of philosophy). Swinburne University of Technology, Australia

Liebermann, D. G., Katz, L., Hughes, M. D., Bartlett, R. M., Mcclements, J., & Franks, I. M. (2002). Advances in the application of information technology to sport performance. Journal of Sports Sciences, 20(10), 755-769. doi:10.1080/026404102320675611

Malacrida, G. (2020). Rowing 101. Retrieved May 3, 2020, from http://www.milehighrowing.org/rowing-101/

Muscles Used. (2019, July 24). Retrieved May 8, 2020, from https://www.concept2.com/indoor-rowers/training/muscles-used

North, C., & Shneiderman, B. (2000). Snap-together visualization: Can users construct and operate coordinated visualizations? International Journal of Human-Computer Studies, 53(5), 715-739. doi:10.1006/ijhc.2000.0418

Parkinson, L. (2020). Rowing injuries. Retrieved January 29, 2020, from http://oakridgephysio.ca/view/lib/rowing-injuries/126

Roberts, J. C. (2007). State of the Art: Coordinated & Multiple Views in Exploratory Visualization. Fifth International Conference on Coordinated and Multiple Views in Exploratory Visualization (CMV 2007). doi:10.1109/cmv.2007.20

Robertson, G., Fernandez, R., Fisher, D., Lee, B., & Stasko, J. (2008). Effectiveness of Animation in Trend Visualization. IEEE Transactions on Visualization and Computer Graphics, 14(6), 1325–1332. doi: 10.1109/tvcg.2008.125

Rowing Basics. (n.d.). Retrieved May 15, 2020, from https://www.rowpnra.org/pnra/rowing-basics/

Shea, C. H., & Wulf, G. (1999). Enhancing motor learning through external-focus instructions and feedback. Human Movement Science, 18(4), 553-571. doi:10.1016/s0167-9457(99)00031-7

Sigrist, R., Rauter, G., Riener, R., & Wolf, P. (2012). Augmented visual, auditory, haptic, and multimodal feedback in motor learning: A review. Psychonomic Bulletin & Review, 20(1), 21-53. doi:10.3758/s13423-012-0333-8

Snodgrass, S. J., Rivett, D. A., Robertson, V. J., & Stojanovski, E. (2010). Real-time feedback improves accuracy of manually applied forces during cervical spine mobilisation. Manual Therapy, 15(1), 19-25. doi:10.1016/j.math.2009.05.011

Swinnen, S. P., Lee, T. D., Verschueren, S., Serrien, D. J., & Bogaerds, H. (1997). Interlimb coordination: Learning and transfer under different feedback conditions. Human Movement Science, 16(6), 749-785. doi:10.1016/s0167-9457(97)00020-1

Todorov, E., Shadmehr, R., & Bizzi, E. (1997). Augmented Feedback Presented in a Virtual Environment Accelerates Learning of a Difficult Motor Task. Journal of Motor Behavior, 29(2), 147-158. doi:10.1080/00222899709600829

US Rowing. (2019). The Stroke. Retrieved October 8, 2019, from http://www.usrowing.org/the-stroke/.

Using the Force Curve. (2019, July 24). Retrieved from https://www.concept2.com/indoor-rowers/training/tips-and-general-info/using-the-force-curve

Vicon Motion Systems. (2016). Plug-in gait reference guide. Retrieved December 12, 2019, from.

Ward, M. O., Grinstein, G., & Keim, D. (2015). 3.5.4 Relative Judgement. In Interactive data

visualization: Foundations, techniques, and applications (2nd ed., pp. 130-132). Boca Raton, FL: CRC Press.

Whitman. (2020). Rowing Terms. Retrieved March 4, 2020, from https://www.whitmancrew.org/terms

Wishart, L. R., Lee, T. D., Cunningham, S. J., & Murdoch, J. E. (2002). Age-related differences and the role of augmented visual feedback in learning a bimanual coordination pattern. Acta Psychologica, 110(2-3), 247-263. doi:10.1016/s0001-6918(02)00036-7

Wulf, G., Hörger, M., & Shea, C. H. (1999). Benefits of Blocked Over Serial Feedback on Complex Motor Skill Learning. Journal of Motor Behavior, 31(1), 95-103. doi:10.1080/00222899909601895

Wulf, G., Shea, C. H., & Matschiner, S. (1998). Frequent Feedback Enhances Complex Motor Skill Learning. Journal of Motor Behavior, 30(2), 180-192. doi:10.1080/00222899809601335

Appendices

Appendix A

*DDR data was noisy (and therefore did not provide accurate data)

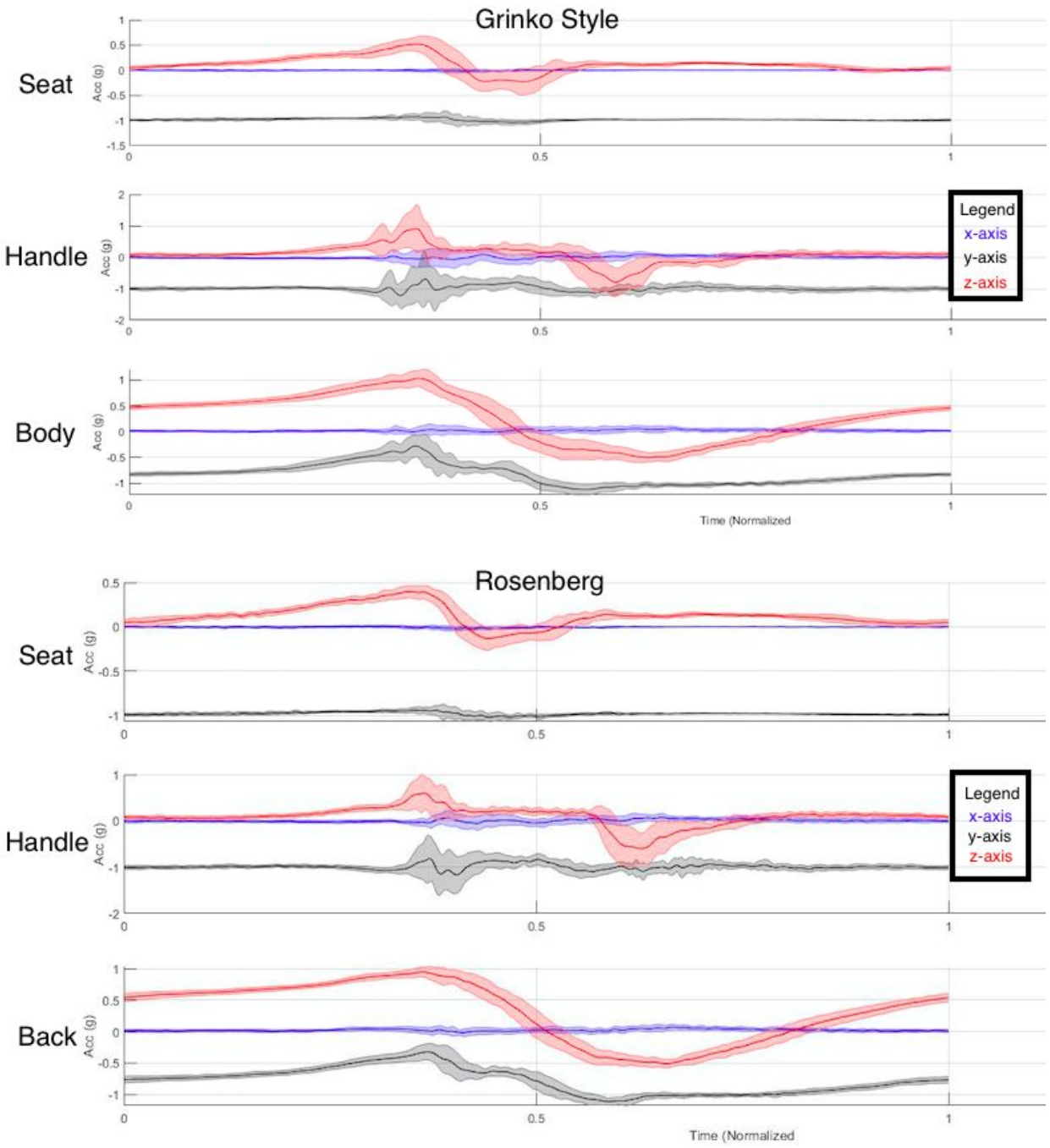

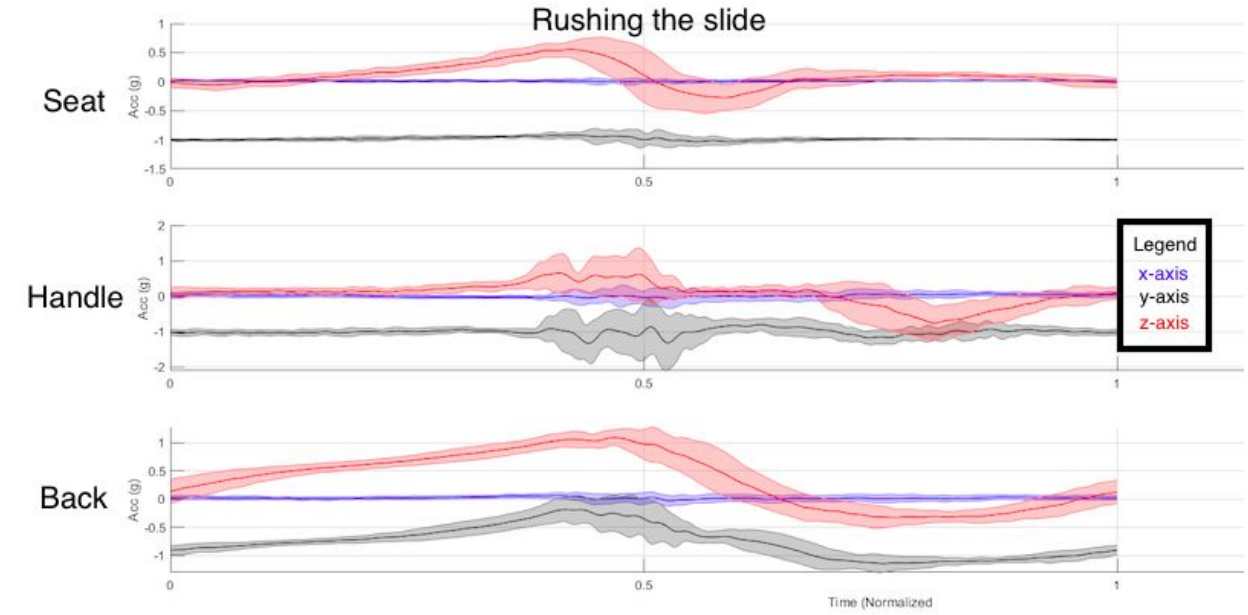
Rushing the slide
Seat
Handle
Back
Acc (g)
Time (Normalized
Legend
x-axis
y-axis
z-axis

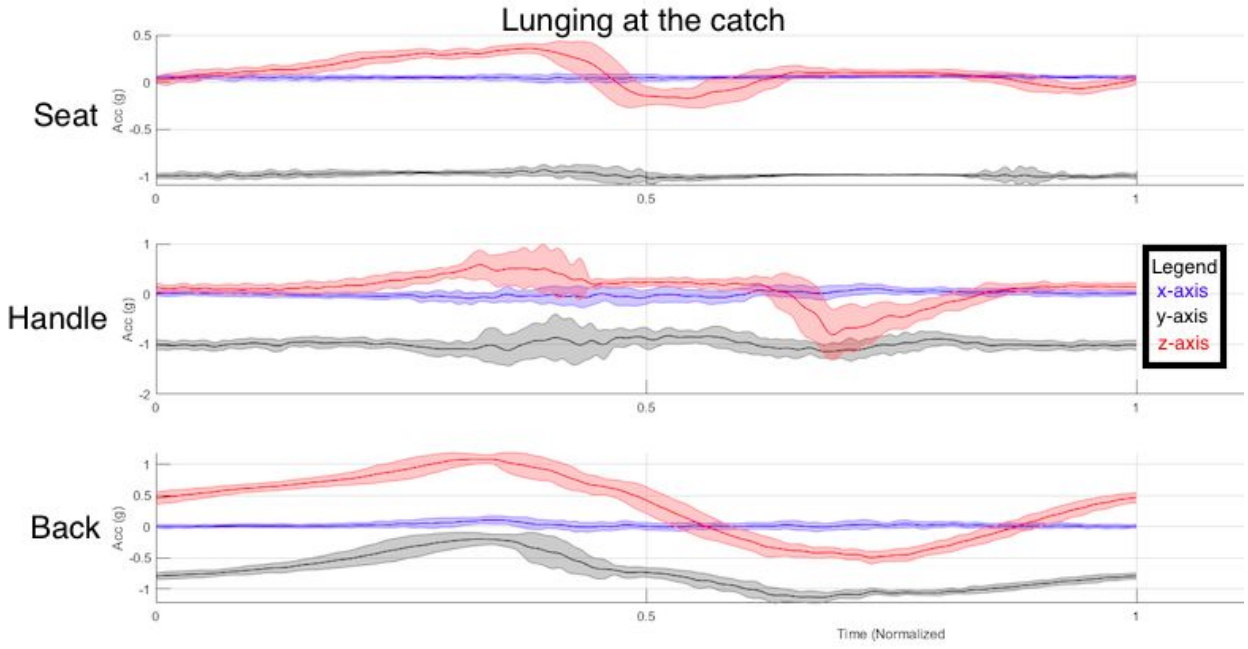
Lunging at the catch
Seat
Handle
Back
Acc (g)
Time (Normalized
Legend
x-axis
y-axis
z-axis

Appendix B

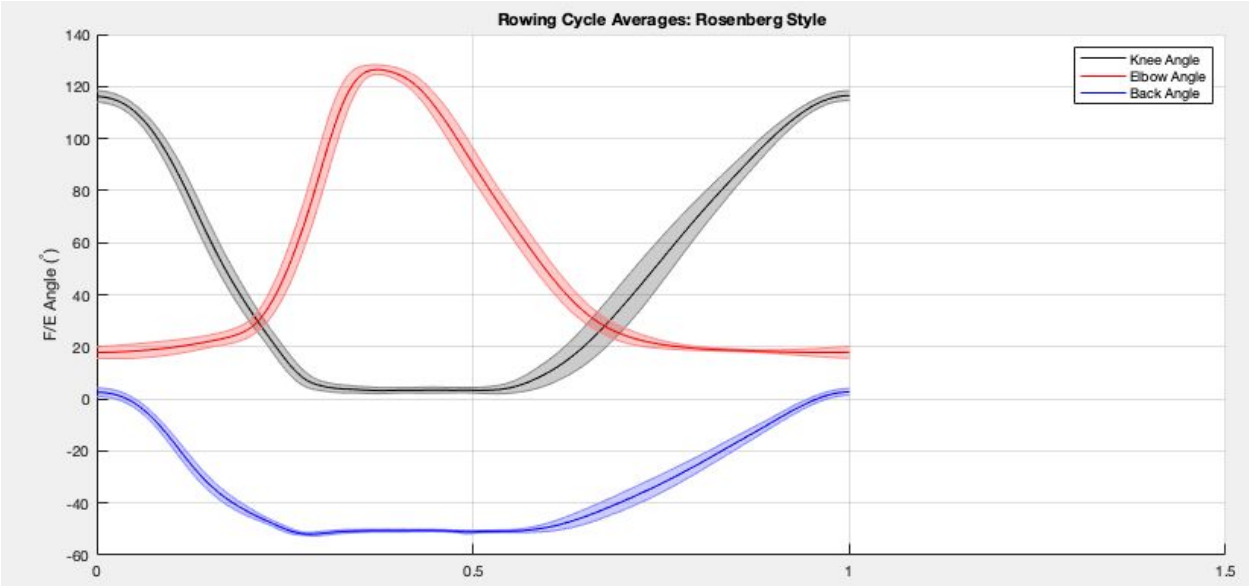
Rowing Cycle Averages: Rosenberg Style
Knee Angle
Elbow Angle
Back Angle
F/E Angle (°)
140
120
100
80
60
40
20
0
-20
-40
-60
0
0.5
1
1.5

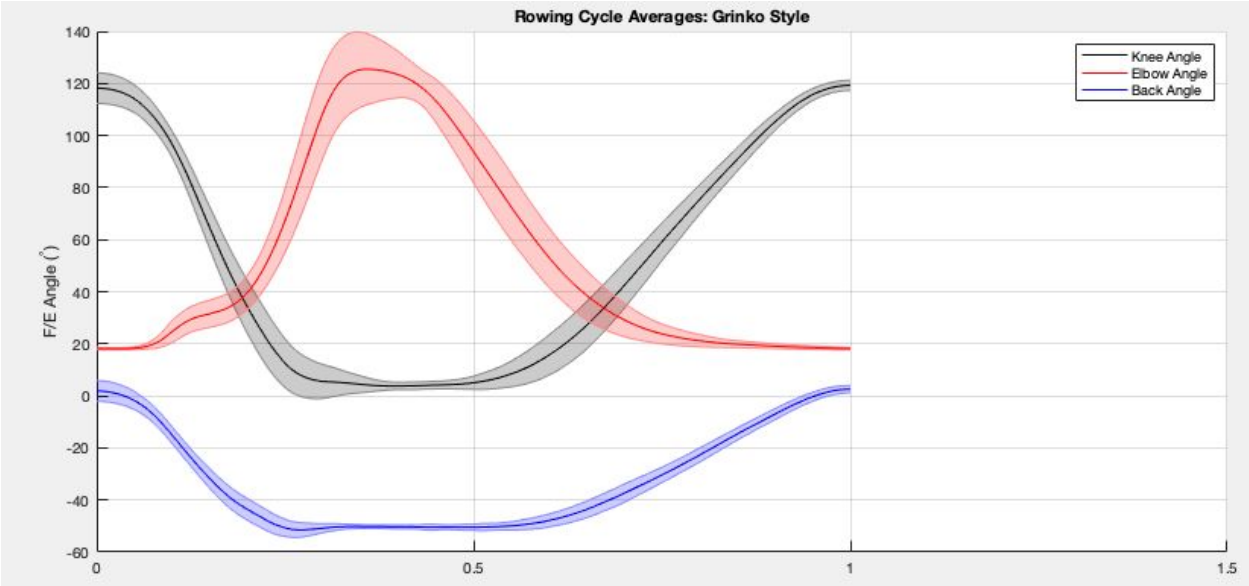
Rowing Cycle Averages: Grinko Style
Knee Angle
Elbow Angle
Back Angle
F/E Angle (°)
140
120
100
80
60
40
20
0
-20
-40
-60
0
0.5
1
1.5

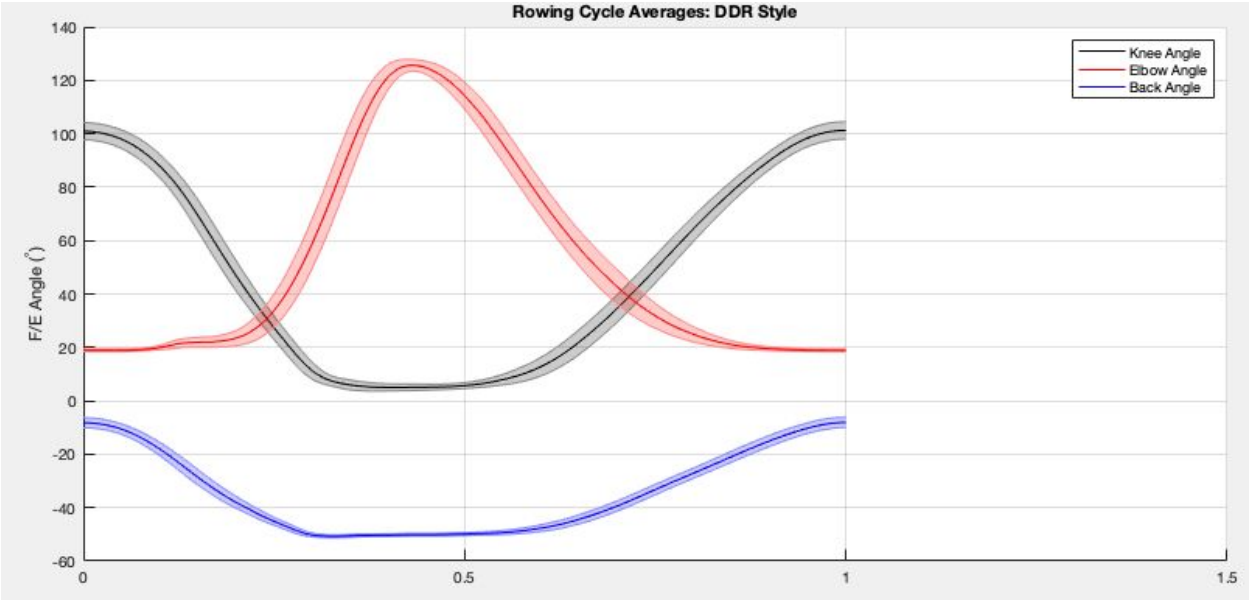
Rowing Cycle Averages: DDR Style
Knee Angle
Elbow Angle
Back Angle
F/E Angle (°)
140
120
100
80
60
40
20
0
-20
-40
-60
0
0.5
1
1.5

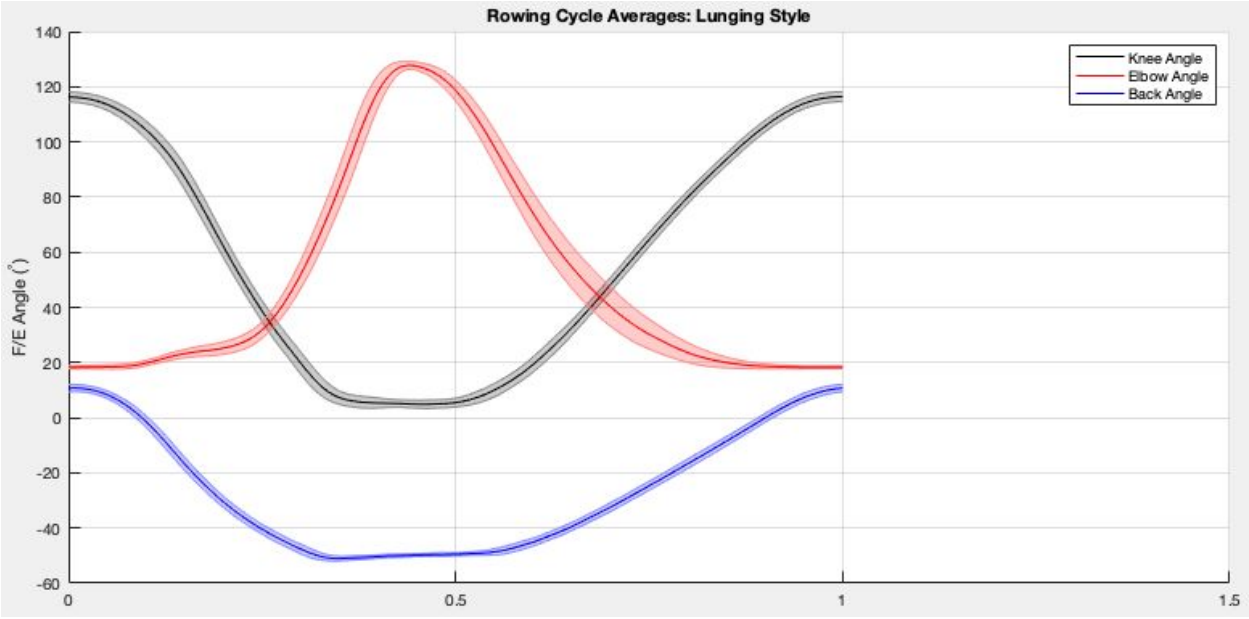
Rowing Cycle Averages: Lunging Style
Knee Angle
Elbow Angle
Back Angle
F/E Angle (°)
140
120
100
80
60
40
20
0
-20
-40
-60
0
0.5
1
1.5

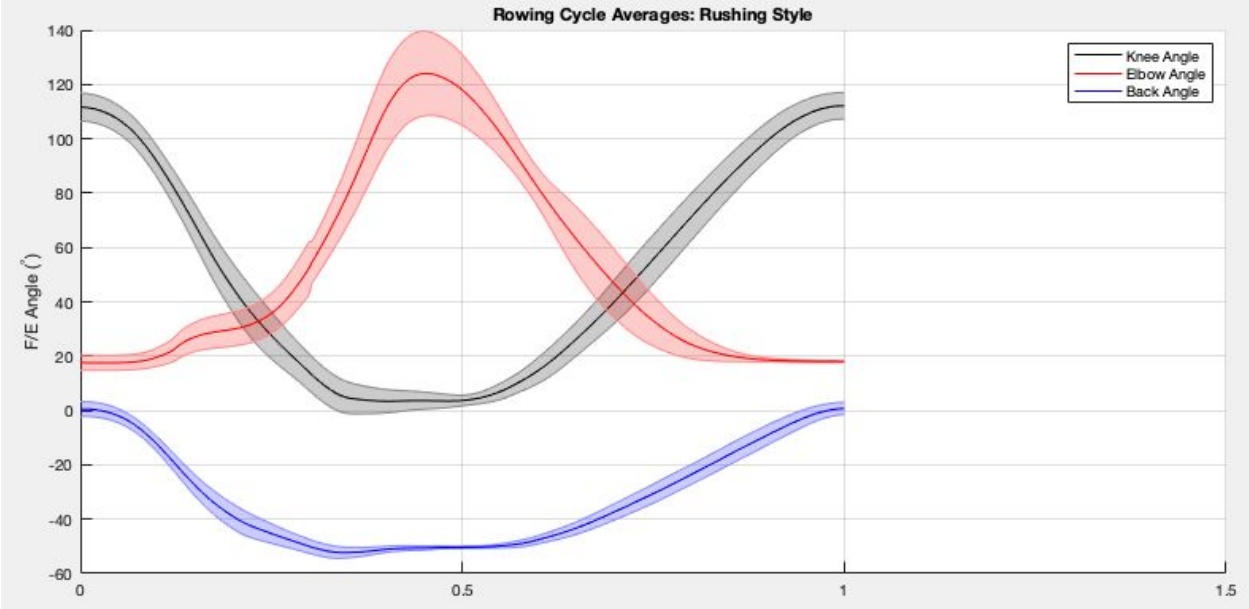
Rowing Cycle Averages: Rushing Style
Knee Angle
Elbow Angle
Back Angle
F/E Angle (°)
140
120
100
80
60
40
20
0
-20
-40
-60
0
0.5
1
1.5

Appendix C

This is the script for the creation of the position graphs.

Load the study data

```
KinematicData =
csvread('ShootingTheSlide.csv',5,0,'A6..OK10000'); %csvread('FileName',start
row, start column, 'spreadsheet range')
IMUData =
csvread('ShootingTheSlide_Plot_and_Store_Rep_1.7.csv',1,0);
```

Define some variables

```
MocapFrameRate = 100; %Samples/second
RowingStyle = 'Rushing'; %Indicate the rowing style to title the
```

Sort into relevant variables and make data equal length.

```
IMUTime = IMUData(:,3);
% The IMU Data is padded with zeros at the end, find the point at
Which the timer stops and remove the extra zeros
[CaptureLength,I] = max(IMUTime);
IMUData = IMUData(1:I,:);
IMUTime = IMUTime(1:I);
% Create a time vector for the motion capture data based on the IMU Time and the length of the mocap data
MocapTime = linspace(0,CaptureLength,length(KinematicData));
% Sort out the relevant kinematic measurements from the data
KneeAngle_R = KinematicData(:,300); %Rotation about x (flexion/extension)
KneeAngle_L = KinematicData(:,108); %Rotation about x (flexion/extension)
ElbowAngle_R = KinematicData(:,234:236);
ElbowAngle_L = KinematicData(:,42:44);
PelvisAngle_R = KinematicData(:,351);
PelvisAngle_L = KinematicData(:,159);

% Use the matlab function interp1 so that the IMU data and motion capture data share the same time vector

KneeAngle_R = interp1(MocapTime,KneeAngle_R,IMUTime);
KneeAngle_L = interp1(MocapTime,KneeAngle_L,IMUTime);
ElbowAngle_R = interp1(MocapTime,ElbowAngle_R,IMUTime);
ElbowAngle_L = interp1(MocapTime,ElbowAngle_L,IMUTime);
PelvisAngle_R = interp1(MocapTime,PelvisAngle_R,IMUTime);
PelvisAngle_L = interp1(MocapTime,PelvisAngle_L,IMUTime);
% Rename the IMU time to the single time vector
Time = IMUTime;
```

Plot the unprocessed data to check its quality

```
%Plot the kinematic data on one figure
figure
subplot(3,1,1)
hold on
grid on
plot(Time, KneeAngle_R)
plot(Time, KneeAngle_L)
title('Knee Angle')
```

```
ylabel('Flexion/Extension (^\circ)')
subplot(3,1,2)
hold on
grid on
plot(Time, ElbowAngle_R)
plot(Time, ElbowAngle_L)
title('Elbow Angle')
ylabel('Flexion/Extension (^\circ)')
subplot(3,1,3)
hold on
grid on
plot(Time, PelvisAngle_R)
plot(Time, PelvisAngle_L)
title('Back Angle')
ylabel('Flexion/Extension (^\circ)')
xlabel('Time (s)')
```

Fill in Gaps in the motion capture data and filter the IMU data

```
% Use a cubic spline interpolant to fill gaps in the kinematic data
KneeAngle_R(:,1) = gapfiller(KneeAngle_R(:,1));
KneeAngle_L(:,1) = gapfiller(KneeAngle_L(:,1));
ElbowAngle_R(:,1) = gapfiller(ElbowAngle_R(:,1));
ElbowAngle_L(:,1) = gapfiller(ElbowAngle_L(:,1));
PelvisAngle_R(:,1) = gapfiller(PelvisAngle_R(:,1));
PelvisAngle_L(:,1) = gapfiller(PelvisAngle_L(:,1));
```

Find the repetitions in the exercise based off the knee angle

```
% Seperate function that searches for the points of maximum knee flexion, these points are used to segment the rowing repetitions
[RepIndexes] = findreps(KneeAngle_R(:,1), 40, 70);
```

Segment the data into individual repetitions

```
% Initialize a variable that tracks the number of samples in each repetition
RepetitionLengths = [];
% Iterate through the repetition indexes to segment the data into
% individual repetitions
for i = 1:length(RepIndexes)-1
SegmentedKneeAngles{i} = [KneeAngle_R(RepIndexes(i):RepIndexes(i
+1),1),KneeAngle_L(RepIndexes(i):RepIndexes(i+1),1)];
SegmentedElbowAngles{i} = [ElbowAngle_R(RepIndexes(i):RepIndexes(i
+1),1),ElbowAngle_L(RepIndexes(i):RepIndexes(i+1),1)];
SegmentedPelvisAngle{i}= [PelvisAngle_R(RepIndexes(i):RepIndexes(i
+1),1),PelvisAngle_L(RepIndexes(i):RepIndexes(i+1),1)];

RepetitionLengths = [RepetitionLengths;length(SegmentedKneeAngles{i}(:,1))];
End
```

Normalize each repetition and interpolate so they share the same time vector

```
LongestRepetition = max(RepetitionLengths);
NormalizedTime = linspace(0,1,LongestRepetition);
for i = 1:length(RepetitionLengths)
RepTime = linspace(0,1,length(SegmentedKneeAngles{i}(:,1)));
```

```
NormalizedKneeAngle_R(:,i) =
interp1(RepTime,SegmentedKneeAngles{i}(:,1),NormalizedTime);
NormalizedKneeAngle_L(:,i) =
interp1(RepTime,SegmentedKneeAngles{i}(:,2),NormalizedTime);
NormalizedElbowAngle_R(:,i) =
interp1(RepTime,SegmentedElbowAngles{i}(:,1),NormalizedTime);
NormalizedElbowAngle_L(:,i) =
interp1(RepTime,SegmentedElbowAngles{i}(:,2),NormalizedTime);
NormalizedPelvisAngle_R (:,i)=
interp1(RepTime,SegmentedPelvisAngle{i}(:,1),NormalizedTime);
NormalizedPelvisAngle_L(:,i) =
interp1(RepTime,SegmentedPelvisAngle{i}(:,2),NormalizedTime);
end

for i = 1:length(NormalizedTime)
% Calculate the average knee angles across all repetitions
AverageKneeAngle_R(i) = mean(NormalizedKneeAngle_R(i,:));
AverageKneeAngle_L(i) = mean(NormalizedKneeAngle_L(i,:));
% Calculate the standard deviation of the knee angle across all
% repetitions
SigmaKneeAngle_R(i) = std(NormalizedKneeAngle_R(i,:));
SigmaKneeAngle_L(i) = std(NormalizedKneeAngle_L(i,:));
% Calculate the average elbow angles across all repetitions
AverageElbowAngle_R(i) = mean(NormalizedElbowAngle_R(i,:));
AverageElbowAngle_L(i) = mean(NormalizedElbowAngle_L(i,:));
% Calculate the standard deviation of the elbow angle across all
% repetitions
SigmaElbowAngle_R(i) = std(NormalizedElbowAngle_R(i,:));
SigmaElbowAngle_L(i) = std(NormalizedElbowAngle_L(i,:));
% Calculate the average thorax angles across all repetitions
AveragePelvisAngle_R(i) = mean(NormalizedPelvisAngle_R(i,:));
AveragePelvisAngle_L(i) = mean(NormalizedPelvisAngle_L(i,:));
% Calculate the standard deviation of the elbow angle across all
% repetitions
SigmaPelvisAngle_R(i) = std(NormalizedPelvisAngle_R(i,:));
SigmaPelvisAngle_L(i) = std(NormalizedPelvisAngle_L(i,:));
end
```

Plot the average of each sensor and kinematic measurement

```
figure
hold on
shadedErrorBar(NormalizedTime,AverageKneeAngle_R,SigmaKneeAngle_R,'lineProps','-
k');
shadedErrorBar(NormalizedTime,AverageElbowAngle_R,SigmaElbowAngle_R,'lineProps','-
r');
shadedErrorBar(NormalizedTime,AveragePelvisAngle_R,SigmaPelvisAngle_R, 'lineProps','-
b');
grid on
xlim([0,1.5])
legend('Knee Angle','Elbow Angle','Back Angle')
ylabel('F/E Angle (^\circ)')
title(['Rowing Cycle Averages: ',RowingStyle,' Style'])
```